ABSTRACT

Title of Document:	MICROFLUIDIC ASSAY PERFORMANCE ENHANCEMENT USING POROUS VOLUMETRIC DETECTION ELEMENTS FOR IMPEDEMETRIC AND OPTICAL SENSING
	Michael Sean Wiederoder, PhD, 2016
Directed By:	Professor Don L. DeVoe Department of Mechanical Engineering

Microfluidic technologies have great potential to help create automated, cost-effective, portable devices for rapid point of care (POC) diagnostics in diverse patient settings. Unfortunately commercialization is currently constrained by the materials, reagents, and instrumentation required and detection element performance. While most microfluidic studies utilize planar detection elements, this dissertation demonstrates the utility of porous volumetric detection elements to improve detection sensitivity and reduce assay times.

Impedemetric immunoassays were performed utilizing silver enhanced gold nanoparticle immunoconjugates (AuIgGs) and porous polymer monolith or silica bead bed detection elements within a thermoplastic microchannel. For a direct assay with 10 µm spaced electrodes the detection limit was 0.13 fM AuIgG with a 3 log dynamic range. The same assay was performed with electrode spacing of 15, 40, and 100 µm with no significant difference between configurations. For a sandwich assay the detection limit was 10 ng/mL with a 4 log dynamic range. While most impedemetric assays rely on expensive high resolution electrodes to enhance planar

senor performance, this study demonstrates the employment of porous volumetric detection elements to achieve similar performance using lower resolution electrodes and shorter incubation times.

Optical immunoassays were performed using porous volumetric capture elements perfused with refractive index matching solutions to limit light scattering and enhance signal. First, fluorescence signal enhancement was demonstrated with a porous polymer monolith within a silica capillary. Next, transmission enhancement of a direct assay was demonstrated by infusing aqueous sucrose solutions through silica bead beds with captured silver enhanced AuIgGs yielding a detection limit of 0.1 ng/mL and a 5 log dynamic range. Finally, *ex situ* functionalized porous silica monolith segments were integrated into thermoplastic channels for a reflectance based sandwich assay yielding a detection limit of 1 ng/mL and a 5 log dynamic range. The simple techniques for optical signal enhancement and *ex situ* element integration enable development of sensitive, multiplexed microfluidic sensors.

Collectively the demonstrated experiments validate the use of porous volumetric detection elements to enhance impedemetric and optical microfluidic assays. The techniques rely on commercial reagents, materials compatible with manufacturing, and measurement instrumentation adaptable to POC diagnostics.

MICROFLUIDIC ASSAY PERFORMANCE ENHANCEMENT USING POROUS VOLUMETRIC DETECTION ELEMENTS FOR IMPEDEMETRIC AND OPTICAL SENSING

By

Michael Sean Wiederoder.

Dissertation submitted to the Faculty of the Graduate School of the
University of Maryland, College Park, in partial fulfillment
of the requirements for the degree of
Doctor of Philosophy
2016

Advisory Committee:

Professor Don L. DeVoe, University of Maryland, College Park, Chair
Professor Gregory F. Payne, University of Maryland, College Park
Professor Srinivasa R. Raghavan, University of Maryland, College Park (Dean's Representative)
Professor Qin Wang, University of Maryland, College Park
Professor Ian M. White, University of Maryland, College Park

Acknowledgements

First, I would like to thank my beautiful wife Danielle for her support, love, silliness, and enthusiasm. You inspire me everyday to accomplish great things and be the best person I can be.

I want to thank my advisor Prof. Don DeVoe for his thoughtful mentorship during my PhD studies. You always supported my decisions, guided my work intelligently, and provided opportunities to do exciting, impactful research that will provide a foundation for my future endeavors.

I want to thank my committee members Profs Srinivsan Raghavan, Greg Payne, Qin Wang, and Ian White for their guidance and input in this dissertation. I especially want to thank Prof White for letting me rotate in his lab and co-teach his biosensors course during my studies.

Many thanks to the members of the Maryland MEMS and Microfluidics Laboratory and my Bioengineering classmates for their support, friendship, and collaborative conversations. I especially want to recognize those who contributed to the work presented in this dissertation including Eric Kendall, Annie Lu, Omid Rahmanian, Luke Peterken, Jin-Hee Han and Isaac Misri.

I want to thank my family for their love and support. I especially want to thank my parents for their influence, for letting me fail, and for giving me all the opportunities to pursue my dreams.

Finally there are many other parties that influenced my studies at the University of Maryland that merit recognition. To my previous research mentors Y. Martin Lo, Bradley Marks, Evangelyn Alocilja, Klint Rose, and Maxim Shusteff. To ESPN for shutting down Grantland just as I started writing my dissertation. To the Graduate Student Government for teaching me how good engineers have it, helping me learn about university politics and supporting all the graduate students they represent. To all federal taxpayers for supporting my research and salary. To the UMD graduate school and A James Clark School of Engineering for funding my travel. To the musical artists that inspired both my experiments and the equipment I used (it's a real thing Kate) including but not limited to D'Angelo, D'Angelo and the Vanguard, Stevie Wonder, Kings of Leon, the Beastie Boys, the Replacements, David Bowie, the Fancy Werewolves, Amy Winehouse, the Rolling Stones, Lauren Hill, the Jackson 5, the Spartan Dischords, Sturgill Simpson, Vampire Weekend, The Who, Miranda Lambert, Eric Church, Prince (RIP), Otis Redding, and Wilco. To my sports teams including Math Madness, Tuesday Night Dinners, the Artful Dodgers, the Smith Business School, the UMD graduate ultimate frisbee group and Spartan FC. To the Maryland Gospel Choir and Joyful Noise for nurturing my musical and spiritual

self. Finally in no particular order a shout out to the DC Gentleman, the MML whiskey club, Werewolf Wednesdays, the Flying Squirrel Fantasy Football League, alliterative e-mails, the Yuk, Sigma Alpha Nu for the Starbucks gift card, the Humble Walk, Tom Izzo, Mark Dantonio, beating Duke, the MSU Biosensors Laboratory, Founder's, Bell's, Bald Eagle t-shirts, sloths, the occasional coffee, fixed roof leaks, properly labeled chemical waste, Sam Kendall's artwork, inappropriately projected anatomical pictures for bioimaging class, BGSS pizza, the UMD FabLab staff, ginger beards, "camping", Town Hall, Truckeroo, clown questions bro, oysters on Prozac, Chelsea FC, GradProm, Walker Texas Ranger, the Wiz, band photos, your pocketbooks and your wallets, staring contests, more cowbell, fish ties, March Madness at Looney's, Trivia night, climbing trees, and laser tag.

Table of Contents

List of Figures

Chapter 1: Introduction

1.1 Background

In the earliest days of medicine, health care was delivered in a patient's home by a traveling physician. However, as new medical technologies were created in the twentieth century health care transitioned to specialized hospitals that utilized large centralized laboratories for cost effective analysis of patient samples.[1] These centralized laboratories were equipped with air-conditioning, refrigerated chemical storage, a constant supply of reagents, reliable electrical power, and highly-trained personnel.[2] Now as the twenty-first century begins modern health care is yet again in the midst of a paradigm shift back to delivering health care to the patient in a diverse array of environments and not just at centralized facilities. Because of technological innovations diagnostics is now increasingly being done in these point of care (POC) locations to provide continuous, rapid, personalized results to improve healthcare outcomes for a patient.[1] With these tests a health care professional or the patient themselves can diagnose diseases quicker than current methods, help manage chronic conditions, monitor reactions to treatment, and participate in epidemiological studies across a large sample for research studies.[1] This emphasis on POC testing is also expanding access to medical diagnostics worldwide by making tests more affordable, efficient, and compatible with resource limited environments such as underdeveloped countries, remote geographical areas, or military battlefields that may not have well developed infrastructure.[3,4] The technology has applications in fields such as food safety and environmental monitoring that also rely mainly on sample analysis in

centralized laboratories. Given the diversity of applications the ideal POC diagnostic

test characteristics such as cost, assay completion time, biomarker concentration

sensitivity, detection limit, dynamic range, ease of use, personnel requirements, and

instrumentation required to interpret results are highly dependent on the application

and patient or sample collection setting.[3]

Many researchers focus on lab on a chip (LOC) technologies to develop small,

POC devices to fit into this new health care paradigm. The technology, first pursued

in the early 1990's,[5] can be applied to biological separation science, DNA analysis,

immunology, and clinical diagnostics.[6] These LOC devices utilize microfluidic

technologies to manipulate small fluid volumes within micrometer scale fluid

channels to perform tasks done in existing traditional bench-top assays.[6–9] These LOC

technologies improve on conventional methods by enabling sample volume reduction,

low reagent consumption, rapid analysis times, portability, multiplexed analysis, and

assay automation.[2,10] Despite the promise of LOC technologies there is still an unmet

need for fully-developed commercial POC diagnostic tests.[9] The work in this

dissertation will address some of these limitations by demonstrating novel methods to

enhance the performance of impedemetric and optical microfluidic detection

elements. The demonstrated techniques will utilize porous volumetric detection

elements to improve assay sensitivity and reduce assay times, rely on simple

instrumentation, and use materials compatible with high-throughput manufacturing.

Overall the work presented will provide new methods to improve LOC technologies

for POC diagnostic tests.

1.2 Microfluidic Sensor Technology Limitations for POC settings

The following section will summarize current limitations in the development

of microfluidic technologies for POC diagnostics and suggest methods to overcome

these limitations. Current methods, materials and reagents used for laboratory based

research are often not portable, compatible with mass production, or too expensive to

implement for POC tests.[2] In addition the instrumentation and computational

resources required to interpret results are frequently impractical for POC settings.[2,11]

Finally, many LOC devices simply cannot achieve cost-effective detection or

quantification of low concentration species required for many diagnostic assays. A

need exists for more sensitive microfluidic detection methods for implementation in

POC diagnostic tests.

1.2.1 Advantages of Thermoplastic Materials for Microfluidic Device Construction

The materials used for fabrication represents one significant barrier to

development of POC microfluidic devices.[2] Many LOC devices are made using

traditional microelectromechanical systems (MEMS) fabrication techniques on

silicon or glass substrates that are fragile and too expensive for a POC test.[2,12,13]

Many laboratory based microfluidic devices are made with easy-to-fabricate poly

(dimethylsiloxane) (PDMS) that is permeable to many small and hydrophobic

molecules and not economically viable for high throughput production.[2,10]

Microfluidic assays that rely on capillary driven flow across paper patterned with

hydrophobic channels and reagents is another common technique for inexpensive

POC assays.[11] However these devices are not always robust, have relatively high

detection limits for many popular assays, retain low sample volumes due to

evaporation, and are not compatible with low surface tension fluids such as biological samples with surfactants.[11] In contrast thermoplastics such as polymethylmethacrylate (PMMA), polycarbonate (PC), polystyrene (PS) and cyclic olefin polymers (COP) are attractive because they are inexpensive, robust, and scalable for industrial manufacturing by injection molding or hot embossing.[10,12,13] COP in particular is desirable given its transparency to visible and UV light, low water absorption, biological inertness, minimal gas permeability, resistance to acids, bases, and solvents, mechanical bond strength,[14] and compatibility with injection molding[15] and hot embossing[16] for high-throughput manufacturing. By using COP it is possible to fabricate robust, low-cost, portable POC diagnostic devices.[17]

1.2.2 Need for Improved Electrical Detection Methods

Many microfluidic devices intended for POC applications utilize electrical detection modalities to acquire data in real-time. Common electrical detection techniques include conductometric,[18,19] impedemetric,[19] or magnetoresistance[20] measurements to quantify the biomarker target concentration.[11] Impedance in particular is popular for monitoring detailed changes in induced capacitance and resistance based on biorecognition events.[21,22] While traditional lab-based impedance sensors utilize macrosize electrodes,[23,24] recently developed sensors use interdigitated electrode arrays that maximize electrode surface area and thus increase signal to noise ratio reducing assay completion times, sample volumes, and detection limits.[19,25] The arrays are usually fabricated with gold because it does not oxidize, gives the best signal to noise ratio,[25,26] and can be patterned on silicon,[27] glass,[28,29] or polymers[30] using commercially viable photolithography techniques. While integrating functional

electrode arrays into rigid glass and silicon microchannels require complex fabrication techniques, COP based devices can utilize simple bonding processes adaptable to mass production.[17,30] Thus, it is possible to integrate high surface area gold electrode arrays into COP based POC devices for sensitive and rapid impedance based sensing.

1.2.3 Need for Improved Optical Detection Methods

Many microfluidic devices also rely on optical detection techniques such as fluorescence,[31] chemiluminescence,[32] or colorimetric changes[33] for POC research applications. Colorimetric measurements have particular advantages with respect to optics simplicity and reagent stability compared to fluorescence and chemiluminescence measurements for POC applications. Fluorescence assays use reagents that can degrade or photobleach when not properly stored, require complex optics and detectors, and are sensitive to auto-fluorescent compounds common in biological samples that can cause false positives.[34] Chemiluminescence assays require calibrated photodetectors and expensive reagents with enzymes that are dynamic and change over time limiting quantification and repeatability.[35] In contrast colorimetric assays can use relatively inexpensive reagents that are less sensitive to environmental conditions and results can be interpreted with the naked eye, cellphone camera, CCD, or photodetector depending on the application.[31,36] Despite these advantages the detection limits and sensitivity for colorimetric assays are typically higher than fluorescence and chemiluminescence assays. Thus techniques to improve the performance of colorimetric based assays would represent a major contribution to POC diagnostics research.

5

1.2.4 Advantages of Volumetric Microfluidic Detection Elements

Most microfluidic assays employ various functionalization routes to anchor proteins, peptides, nucleic acids, or other assay-specific capture probes to chemically modified internal microchannel surfaces.[21,37] The use of planar microfluidic channel wall or electrode surfaces for biomarker capture limits assay performance since each channel wall can be functionalized with, at most, a single monolayer of probes. For thermoplastic substrates challenging surface immobilization chemistries also limit the effective capture probe density.[33,38] Researchers have introduced post arrays into thermoplastics that increase the total surface area available for biomarker capture by a factor of 2~5 due to limitations in structure size.[39] In contrast the introduction of a porous, flow-through detection element increases reaction site density by a factor of 100~1000 and reduces the characteristic diffusive length scales between target and capture probe to improve performance.[28,36,37,40] By optimizing the porosity and the pore size the assay speed, reagent volume, and detection limit can decrease compared to similar planar assays as biomarker capture becomes more efficient.

Numerous porous materials have been demonstrated for volumetric capture of biomarkers in microfluidic devices including packed bead beds, hydrogels, polymer monoliths, membranes, paper, and porous silicon.[37] However many of these materials have specific drawbacks that limit performance for microfluidic assays. Flexible materials such as membranes and paper,[41] compressible materials such as hydrogels,[42] and materials that can shrink such as some polymer monoliths[43] are difficult to consistently seal within a microchannel. As a result the fluid does not flow through the porous media but around the volumetric element at the channel wall interface.

Some materials such as hydrogels and polymer monoliths are often polymerized and functionalized *in situ* causing device to device variability that compromises performance across tests.[44] In contras some materials such as beads, membranes, paper, and porous silicon are usually functionalized *ex situ* before the device is formed to minimize variance.[44] For optically based assays light scattering caused by dielectric constant variation between the porous matrix and fluid within the open pores causes strong coupling with incident light, leading to scattering of photons passing through the matrix.[45] This light scattering significantly decreases optical transparency, limiting the probed volume and reducing sensitivity for optically based assays. An ideal porous volumetric detection element should be rigid to maintain an intimate interface with the microchannel wall, have consistent capture probe density from device to device, and limit light scattering for optical detection.

1.2.5 Advantages of Silver Enhancement of Gold Nanoparticle Conjugates

Gold nanoparticles (AuNP's) labeled with biorecognition probes are common as the transduction element for many biological and chemical assays.[46] AuNP conjugates are simple to synthesize, stable, provide high surface area to volume, are easily tunable, can be attached to many ligand types using well characterized surface chemistries, and are commonly used in commercial lateral flow assays.[46–48] When used in an assay the AuNP conjugate has specific affinity and attaches to a biomarker target captured from the test solution by biorecognition probes immobilized in the detection region.[46] To further amplify signal many researchers utilize a silver enhancement step in which silver ions nucleate on the captured AuNP surface in the presence of a reducing agent to create micron scale silver clusters.[49] For colorimetric

detection silver enhancement amplifies the signal change per biorecognition event to lower the detection limit compared assays that use only AuNPs. In fact the detection limit for optical ELISA tests that use silver enhancement are equivalent to similar tests that use expensive and less stable enzymatic or radioactive labels.[49] For microfluidic immunosensors specifically optical detection of silver enhanced, secondary antibody labeled AuNPs has been demonstrated on both planar cyclic olefin polymer (COP)[33,50] and glass surfaces[51] for POC applications (Figure 1.1).
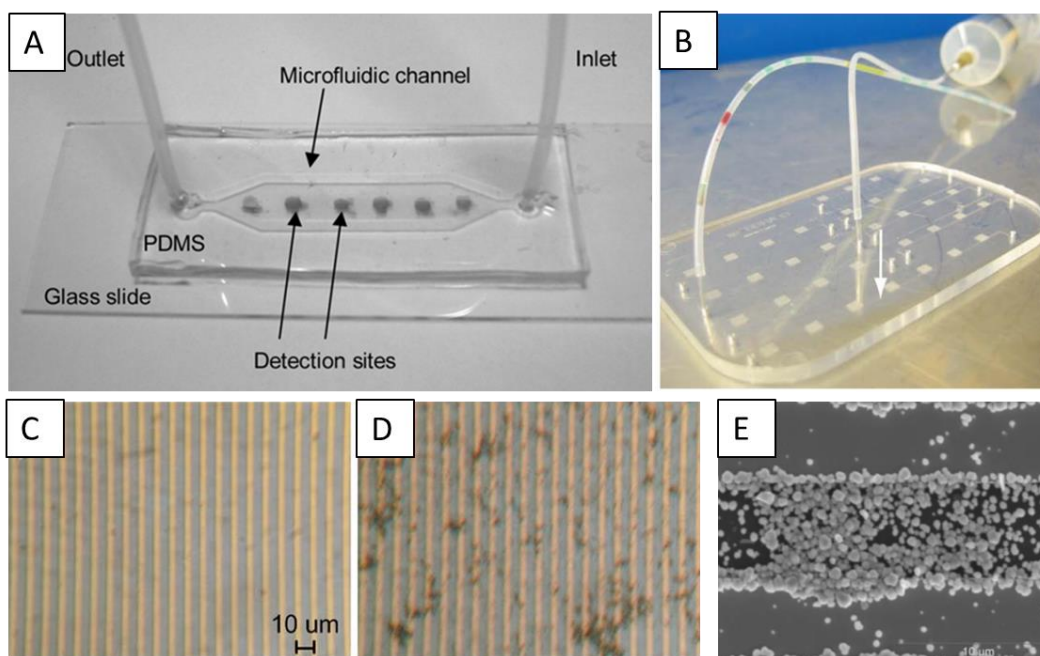
Figure 1.1: Examples of planar based microfluidic devices that employ silver enhancement including optically based sensors that utilize glass and PDMS[51] (A) or cyclic olefin polymer[50] (B) and electrically based sensor that utilizes a gold electrode array (C) and silver enhancement (D)(E)[52].

For electrically based detection the silver enhancement also amplifies signal change by increasing the label probe size for capacitance or resistance measurements.[49] Examples of non-microfluidic sandwich immunoassays utilizing silver enhancement of AuNP's has been demonstrated using IDA's on planar silicon (Figure 1.1)[52] and glass[53–55] surfaces but not thermoplastics. Silver enhancement of AuNP conjugates

represents an inexpensive, stable method to amplify electrical or optical signal for microfluidic assays that has great potential for POC device development.

1.3 Dissertation Approach and Organization

The goal of the research presented in this dissertation is to demonstrate improved sensing performance by employing porous volumetric detection elements in impedemetric and optical microfluidic biosensors. The work will provide new knowledge to the field by quantifying the improvement in assay completion time, dynamic range, and detection limits achieved with porous volumetric sensing elements in contrast to planar detection elements. The work will demonstrate signal amplification for optical and impedance based detection in thermoplastic microchannels using porous volumetric detection elements and silver enhancement of gold nanoparticle conjugates. All investigated techniques will utilize practical methods that are scalable for high-throughput manufacturing, demonstrate signal acquisition compatible with portable instrumentation, and rely on commercially available reagents and instruments. Collectively, the advances reported will provide novel techniques to enhance sensitivity, expand quantification ranges, and lower detection limits for POC tests that utilize microfluidic technology.

The dissertation is organized into five chapters to summarize the work completed. In the following chapter (Chapter 2) volumetric impedance based detection is demonstrated using silver enhancement of AuNP conjugates and an interdigitated electrode array. In contrast to existing planar arrays that require high resolution electrodes to improve sensitivity, this study employs an *in situ* polymerized porous polymer monolith or *ex situ* functionalized silica bead bed in the microchannel

volume that operate successfully independent of the electrode spacing. The formation

of micron scale silver clusters causes an increase in volumetric capacitance and a

decrease in volumetric resistance that correlates with the target concentration in the

tested sample. This novel demonstration suggests methods for easy fabrication of

impedance based sensors for microfluidic devices and demonstrates for the first time

microfluidic volumetric capture elements for impedance based detection.

In Chapter 3, adapted from Wiederoder et al.,[56] optical detection

enhancement of fluorescence and transmission based measurements in porous

volumetric elements is demonstrated by infusing a solution with the same refractive

index as the porous element. The refractive index matching solution minimizes light

scattering caused by refractive index mismatches between the porous element and the

fluid within its pores to enhance optical signal. The technique is demonstrated for a

fluorescence based direct immunoassay using an *in situ* polymerized porous polymer

monolith within a capillary to amplify optical signal 1.6-2.6X by infusing the

monolith monomer. For a colorimetric, transmission based direct immunoassay

aqueous sucrose was infused through a silica bead packed bed containing silver

enhanced AuNP conjugates within a thermoplastic microchannel to achieve a

0.1 ng/mL detection limit and a dynamic range of 5 logs. The experiments show that

the technique is applicable to different types of optical detection, microchannel

material/geometry, and porous media for signal enhancement in microfluidic devices.

Finally, in Chapter 4 optical detection enhancement by infusing index

matching fluid is demonstrated using *ex situ* functionalized porous silica structures

integrated into a thermoplastic microchannel. The porous silica inserts are fabricated

within a thermoplastic mold using a sol-gel process and then functionalized

covalently with antibody capture probes batch-wise to ensure consistency across

devices. The silica inserts are then integrated into a thermoplastic microchannel using

solvent bonding techniques to ensure a tight fluidic seal. A colorimetric, transmission

based direct and sandwich immunoassay utilizing silver enhancement of AuNP

immunoconjugates resulted in detection limits of 1 ng/mL and 10 ng/mL with

dynamic ranges of 5 logs and 4 logs respectively. For a reflectance based colorimetric

sandwich assay the detection limit after AuNP immunoconjugate capture, silver

enhancement, and refractive index matching was 1 µg/mL, 100 ng/mL, and 1 ng/mL

with dynamic ranges of 2, 3, and 5 logs respectively.

Chapter 2: Sensitive Volumetric Impedance Based Microfluidic Sensors using Porous Detection Elements

2.1 Summary

In this chapter impedance based microfluidic biosensors using porous volumetric detection elements are demonstrated to achieve sensitive, rapid detection. While most impedemetric sensors utilize planar capture elements that require high resolution electrodes to concentrate the electric field near surface biorecognition elements, this work instead utilizes porous volumetric elements to monitor biorecognition events in the microchannel volume and enable more efficient target capture. As described in the following sections, thermoplastic microfluidic devices were constructed with either porous polymer monolith or silica bead beds immobilized above a gold interdigitated electrode array to measure volumetric impedance. After gold nanoparticle immunoconjugates (AuIgG) are specifically captured they are silver enhanced to create micrometer scale aggregates that cause a specific decrease in the volumetric impedance. For a direct immunoassay the detection limit was 0.13 fM AuIgG with a 3 log dynamic range after 30 min silver enhancement with no significant difference for electrode arrays with 15, 40, and 100 μm spacing. For a sandwich immunoassay the detection limit was 10 ng/mL with a 4 log dynamic range after 15 min silver enhancement. The results suggest the utilization of less expensive, low resolution electrodes and porous detection elements for volumetric impedance sensing to achieve equivalent or better performance than planar based assays with reduced assay completion times.

2.2 Introduction

Limitations of current point of care (POC) diagnostic tests for patients include long wait-times, a need for centralized laboratories with specific infrastructure, a constant supply of reagents, relatively large sample volumes, and highly-trained personnel.[2] Many researchers are developing micro total analysis systems (μTAS) or "lab-on-a-chip" (LOC) technologies to overcome these problems by utilizing microfluidic technology[9] to perform tasks done in traditional laboratory-based assays on a portable miniaturized device. These LOC devices require smaller sample and reagent volumes, lower production costs, and shorter analysis times than traditional laboratory based assays while allowing for highly sensitive, multiplexed analysis of biological targets.[2,10] Despite this promise greater commercialization of these technologies is limited to laboratory based detection methods that are not translatable to high performance low-cost, portable POC devices.

Impedance spectroscopy (IS) is a popular detection technique for lab on a chip assays because of its sensitivity. Impedemetric biosensors monitor biorecognition events to quantify target concentration based on changes in the capacitive reactance or induced redox reactions near the electrode.[21,22] Traditionally, IS requires macroscale electrodes that are immersed into a sample solution to measure impedance and biomarker concentration.[23,24] In contrast many microfluidic detection devices utilize interdigitated electrode arrays (IDA's) that increase electrode surface area compared to macroscale electrodes.[19,30,57,58] These planar sensors can be made using high-throughput methods such as photolithography to increase sensitivity, reduce assay times and decrease sample volumes compared to macroscale electrodes.[19]

Despite these advantages interdigitated electrode array use is limited by the high costs associated with fabrication of microfluidic devices on materials common for photolithography such as silicon and glass.[59] Recently Zou and others have demonstrated photolithographic deposition of gold electrodes on thermoplastic substrates that are more amenable for high-throughput manufacturing.[30] In addition to optimize detector sensitivity most studies use high resolution (500 nm - 10μm) electrodes using an IDA to concentrate as much of the electric field as possible close to the electrode and substrate surface[60] to probe surface based biorecognition events.[30,58] To realize the advantages of thermoplastic based microfluidic impedemetric sensors new techniques are needed to achieve sensitive detection with less expensive, lower resolution electrodes.

While most developed methods rely on planar impedemetric sensors the capture probe density is limited by the microchannel geometry and functionalization efficiency the biomarker capture is limited.[28] Planar thermoplastic surfaces in particular have low capture probe immobilization efficiencies due to constraints in available chemistries that limit biomarker capture from solution.[28,61] Even when using a nanometer scale IDA to detect IgG on a cyclic olefin polymer (COP) substrate a high detection element of 25 μg/mL was acheived.[30] In contrast to planar capture surfaces, porous flow-through biomarker capture elements can significantly increase reaction site density to reduce assay times and/or increase sensitivity.[40,56] While this has been demonstrated using optical detection[40,56] no known study has used porous, microfluidic volumetric detection elements for impedance based sensing. To solve this problem immunomagnetic concentration of target has been shown in IDA

14

impedance sensors.[62] Unfortunately magnetic particles not attached to target also concentrate in the detection zone and can clump causing a non-specific change in signal.[19] A volumetric capture method that avoids the limitations of planar probe surfaces without amplifying non-specific signals could improve device sensitivity while potentially reducing assay times.

Many studies have also investigated amplification of the change in impedance per binding event using silver enhancement of gold nanoparticle labeled biomarker recognition probes.[49] In the presence of gold and a reducing agent, silver ions nucleate creating large aggregates that modify electrical signal far greater than a gold nanoparticle tagged probe by itself.[49] Numerous microfluidic sensors using optical detection of silver enhanced AuIgG have been demonstrated on thermoplastic[33,63] and glass surfaces[51,56]. However, no known impedance based, flow-through microfluidic sensor has been previously demonstrated using silver enhancement. Non-microfluidic sandwich assays utilizing silver enhancement of AuIgG with IDA's on planar silicon[52] and glass[53–55] surfaces have reported detection limits on the order of 100 fM,[54,55] 10 fM,[53] and 1 fM[52] of biological target. However, these assays require long incubation times (1~2 h) and additional manual processing steps including nitrogen drying and repeated hand pipetting that require trained personnel and developed infrastructure.

The experiments in this study will explore the use of porous volumetric detection elements for impedance based microfluidic sensors employing silver enhanced AuIgG and an IDA for sensitive and rapid detection. The constructed devices utilize either a porous polymer monolith or a silica bead packed bed in a

thermoplastic microfluidic channel. The porous polymer monolith element is polymerized and functionalized both *in situ* (direct immunoassay) and *ex situ* before integration into a microchannel during bonding using a previously developed procedure (sandwich immunoa**s**say)[64]. Silica beads functionalized *ex situ* and packed into a microchannel above an IDA are also utilized for a sandwich immunoassay. The volumetric impedance and phase angle was measured over a frequency before and after formation of silver micrometer-scale aggregates on captured AuIgG. As the silver aggregates form a concentration dependent decrease in the volumetric resistance and capacitive reactance causing a decrease in the measured impedance. For the polymer monolith element a direct immunoassay with a 10 μm electrode gap the detection limit is 0.13 fM AuIgG with a 3 log dynamic range after 30 min silver enhancement. For a direct immunoassay using a polymer monolith and electrode gaps of 15, 40, and 100 μm's no significant difference was observed between tests suggesting that for volumetric impedance based sensors the electrode resolutions has minimal effect on sensor performance with a sufficiently large enough microchannel. For a sandwich immunoassay using a silica bead bed 100 μm electrode spacing the detection limit is 10 ng/mL with a 4 log dynamic range. The constructed device is portable, compatible with high-throughput production, and could be measured using a handheld LCR meter for POC applications.

2.3 Material and Methods

2.3.1 Materials

Glycidal methacrylate (GMA), hydrochloric acid (HCl), cyclohexanol, sodium hydrosulfide, sulfuric acid, 2,2-dimethoxy-2-Phenylacetophenone (DMPA), sodium phosphate dibasic, phosphate buffer saline (PBS), bovine serum albumin (BSA), human IgG, and decalin were purchased from Sigma-Aldrich (St. Louis, MO). Ethoxylated trimethylolpropane triacrylate (SR454) was purchased from Sartomer (Warrington, PA). N-(γ-maleimidobutyryloxy) sulfosuccinimidyl ester (GMBS) was purchased from Thermo Fisher Scientific Inc. (Rockford, IL). NR1-3000PY negative photoresist and RD-6 developer were purchased from Futurrex, Inc. (Franklin, NJ). Silver enhancement solution, anti-human IgG, and 40/60 nm gold nanoparticle tagged anti-human IgG (AuIgG) were purchased from Cytodiagnostics (Burlington, ON). Microfluidic fittings were purchased from IDEX Health & Science (Oak Harbor, WA) and needle tubing was purchased from Hamilton Syringe (Reno, NV).

2.3.2 Electrode Fabrication

The interdigitated electrode array was created via a photolithographic liftoff process demonstrated in a previous study.[30] The procedure for electrode deposition and lift-off was developed by Mr. Isaac Misri. Thermoplastic plaques made with Zeonor1420R or 1020R Cyclic Olefin polymer (COP) Resin (Zeon Chemicals, Louisville, KY) were cut into square pieces before washing with methanol, isopropanol, and deionized water before N_2 drying and overnight degassing at 75 °C. After that NR1-3000PY negative photoresist was spun onto the COP at a thickness of

3.7 μm before UV photo patterning and development in RD-6 developer. Next a 10-20 nm chromium adhesion layer was deposited followed by a 200 nm gold deposition using an e-beam deposition tool. Lift-off was completed in acetone to create an interdigitated electrode array of 10 μm wide fingers with gaps between 10-200 μm's.

2.3.3 Chip Fabrication

The mating COP side was cut to the desired size before channels and fluidic access ports were milled with a 3-axis desktop CNC milling machine (MDX-650, Roland DGA, Irvine, CA) and sonicated in deionized water to remove debris. The milled side and unmilled mating side were then washed with methanol, isopropanol, and deionized water before N_2 drying and overnight degassing at 75 ˚C. The device was then solvent bonded using decalin based on a previously developed procedure.[65] Briefly the channel side was exposed to a decalin in ethanol mixture (w/w), rinsed with ethanol and nitrogen gas, and manually aligned before pressing with the mating side by hand. The multilayer chip was then pressed at 200 psi at 30 ˚C in a hot press (AutoFour/15, Carver, Inc., Wabash, IN) to complete the bonding. Fluidic interfaces for off chip syringe pumps were created by inserting needle tubing segments into the access ports[66] and attaching fluidic fittings.

2.3.4 Direct Assay Procedure

A direct assay was done using silver enhancement of immobilized AuNP antibody conjugates captured within a porous volumetric polymer monolith (Figure 2.1). GMA monolith was formed in the thermoplastic microchannel using a previously described procedure.40 The pre-monolith solution of GMA, ethoxylated trimethylolpropane

triacrylate (SR454), cyclohexanol, and methanol containing a photoinitiator (DMPA) was infused into the channel. The channel was then masked with black tape and exposed to UV light to polymerize the monolith. The channel was subsequently flushed with 100% methanol and 20% methanol and infused with 2 M sodium hydrosulfide in a methanol-0.1M aqueous sodium phosphate dibasic solution for 2 h to transform epoxide groups to thiol groups. Remaining epoxide groups were hydrolyzed by soaking in 0.5M sulfuric acid overnight at 65 ˚C before rinsing with deionized water and ethanol. A 2 mM GMBS solution in ethanol was then infused for 1 h to create an amine functional group. The monolith was then functionalized with 50 μg/mL human IgG or rabbit IgG in 1x PBS and rinsed with 2 mg/mL bovine serum albumin (BSA) in PBS for 15 min to block any unreacted sites before overnight storage at 4˚C.
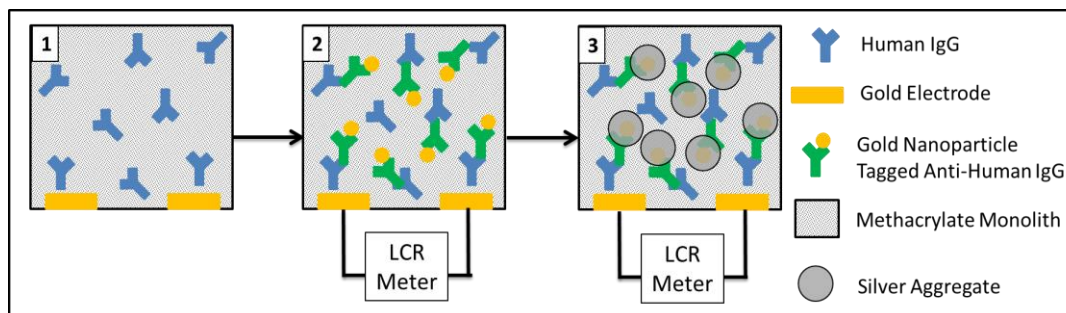
Figure 2.1: Immunosensor procedure schematic. Human IgG is covalently attached to methacrylate monolith (1) and gold nanoparticle tagged antibodies (Au-Abs) are captured during infusion (2). Silver enhancement solution perfuses through monolith region and silver nucleates on gold nanoparticles decreasing impedance measured across gold interdigitated electrodes by an LCR meter due to increasing total capacitance of the channel volume.

After warming to room temperature, the monolith capture region was rinsed for 10 min with 1x PBS, infused with serial dilutions of 40 nm gold nanoparticles tagged with anti-human IgG in 2 mg/mL BSA in PBS for 15 min, and rinsed for 10

19

min with 1x PBS. Next the monolith regions were infused with silver enhancement solution for 15 min, rinsed for 10 min with 1x PBS, silver enhanced an additional 15 min, and rinsed for 10 min with 1x PBS. The silver nitrate and hydroquinone silver enhancement solutions were combined with PBS in an off-chip 4 way junction for infusion. The chips were connected to an LCR meter (4284A, Agilent Technologies, Santa Clara, CA) using a probe station and micropositioners to contact the gold contact pads covered with conductive silver ink (Circuit works, Santa Monica, CA). The LCR meter was controlled with an open-source VI using Labview 7 (National Instruments, Austin, TX) to log the impedance and phase angle between 100 Hz and 1 MHZ at 6 points per decade with 50 mV AC voltage input during PBS rinsing steps before and after Au-Ab infusion and after each silver enhancement step. The interdigitated electrode array consisted of 20 electrode fingers 10 μm in width spaced 10 μm apart. The experiments were also completed using interdigitated electrode arrays consisting of 10 μm fingers and gaps of 15, 40, and 100 μm's using 40 nm AuNP's tagged with anti-rabbit IgG.

2.3.5 Sandwich Assay Procedure: Polymer Monolith

The sandwich assay procedure was similar to the direct assay except for some methods altered to optimize results. The GMA monolith was synthesized using a trapezoidal mold and reintegrated into the final device based on a previously reported procedure for device consistency.[64] Briefly the pre-monolith solution was infused into a milled COP channel capped with black electrical tape, exposed to UV light, removed from the mold, and rinsed with methanol under agitation overnight. The GMA monolith sections were then soaked in 2 M sodium hydrosulfide in methanol-

0.1M aqueous sodium phosphate dibasic solution for 2 h under agitation and rinsed with 20% methanol. The monolith sections were then soaked in 0.5 M sulfuric acid overnight at 65 ˚C before rinsing with deionized water and ethanol. The functionalized monolith segments were then cut to 1 mm lengths for reintegration with a razor blade. After exposing the milled COP side in 35% decalin as described above the monolith segment was positioned into the channel using a wet finetip brush. The electrode side was then manually aligned before insertion into the hot press. Then needle inlet ports were created and the monolith was functionalized by infusing 2 mM GMBS in ethanol for 1 h and 50 μg/mL anti-human IgG in 1x PBS for 1 h. Finally 2 mg/mL BSA in 1X PBS was infused for blocking and the device was stored overnight at 4 ˚C.

For the sandwich immunoassay procedure the non-specific silver enhancement was reduced by combining the 2-part solution on chip and by selecting 0.1X PBS to reduce the number of Cl⁻ ions that can trigger non-specific silver aggregation. The room-temperature device was flushed for 15 min with PBS through the three entrance channels before infusion of serial dilutions of human IgG and 2 mg/mL BSA (control) in PBS for 30 min followed by a 15 min rinse with 0.1X PBS. Next 60 nm gold nanoparticles functionalized with anti-human IgG (Cytodiagnostics, Burlington, ON) diluted 1:50 (v/v) in 2 mg/mL BSA in PBS were infused for 15 min followed by a 15 min 0.1x PBS rinse. Finally the silver enhancement solutions were infused for 20 min before a 15 min 0.1x PBS rinse. The impedance and phase angle were measured before and after AuIgG infusion, during silver enhancement, and after silver enhancement during 0.1X PBS rinsing. The

interdigitated electrode array consisted of 20 electrode fingers 10 μm in width spaced 15 μm apart.

2.3.5 Sandwich Assay Procedure: Silica Bead Bed

A sandwich assay was also completed using a silica bead bed above interdigitated electrode arrays consisting of 6 electrode fingers 10 μm wide spaced 100 μm apart. The silica beads in a 5% wt. aqueous solution were functionalized with amine groups based on a previously reported method.[67] The beads were washed in piranha solution for 1 h before rinsing three times with deionized water and ethanol. Amine groups were introduced by incubating the beads in a solution of 5% (3-aminopropyl) triethoxysilane (APTES), 5% deionized water, and 90% ethanol (v/v) under agitation for 1 h at room temperature and washed 3 times with ethanol and PBS. Human IgG was attached to the beads using BS3, a homobifunctional amine-reactive crosslinker, by combining 400 μL of 500 μg/mL human IgG in 1x PBS, 2 mL of bead solution, and 210 μL of 7.19 mM BS3 in deionized water and incubating 30 min under agitation at room temperature. The reaction was quenched by adding 200 μL of 1 M tris buffer before agitating for 15 min at room temperature. The resulting mixture was washed 3 times with PBS and suspended in 2 mg/mL BSA in PBS overnight at 4 ˚C. Functionalized beads were packed into a microfluidic device using vacuum through the side access channel into the restricted sensing region using a syringe and needle in the fluidic outlet port. Fluidic interfaces for off chip syringe pumps were created by inserting needle tubing segments into the access ports following a previously reported method[66] after the packed bed was formed. Fluidic fittings were attached to the needles and tests were conducted immediately.

For the assay the device was brought to room temperature and infused with 2 mg/mL BSA in 1x PBS for 10 min before infusing serial dilutions of rabbit anti-human IgG for 15 min at 2 μL/min and rinsing with 2 mg/mL BSA in 1x PBS for 10 min. Next, 40 nm AuNP-labelled anti-rabbit IgG solution was diluted 1:50 (v/v) in HEPES buffer containing 1% BSA and 0.05% Tween 20 and infused for 15 min at 2 μL/min, followed by rinsing with 1x PBS for 15 min at 2 μL/min to remove unbound sample. Silver enhancement solution was prepared using a two part mixture[68] chosen due to its stability under light exposure, consisting of 5.0 mg silver acetate in 5 mL deionized water and 12.5 mg hydroquinone in 5 mL citrate buffer at pH 3.8. The silver enhancement solution was infused 15 min after combination an off chip junction and followed by a 10 min rinse with 1x PBS at 2 μL/min. The impedance and phase angle were measured as previously described before and after silver enhancement during infusion with 1x PBS.

Images of the chips before and after assay completion were captured using a color CCD camera (DFK 41AU02, The Imaging Source, Charlotte, NC). Reflectance images were captured by illuminating the chips with a 150 W ring illuminator light source (Fiber-Lite 180 Illuminator, Dolan-Jenner Industries, Boxborough, MA) attached to a stereoscope (S8 APO, Leica Microsystems, Buffalo Grove, IL). Each chip was positioned with its lower surface 2 mm above a cleanroom cloth (Texwipe TechniCloth Nonwoven Dry Wiper, Fisher Scientific, Pittsburgh, PA) which served to provide a uniform white background with low specular reflection for imaging. Images were captured in an episcopic configuration.

For both transmission and reflection measurements, Images were analyzed using Image J software. The region of interest (ROI) used to determine the intensity of the silica bead bed was 300 μm by 600 μm in area, and positioned approximately 200 μm downstream from the entrance. This region of interest excludes the sloped sidewalls to ensure consistent optical measurements across samples. In instances where bubbles were observed to form during sucrose infusion, regions containing bubbles were omitted from analysis.

2.4 Results and Discussion

2.4.1 Device Fabrication

The completed device electrodes have a minimum feature resolution of 5 μm and the electrodes remained undamaged during device bonding as the solvent exposed COP deformed around the electrodes. This overcomes a common problem of electrodes breaking or causing leaks during microfluidic device bonding.[17] In Figure 2.2A an electrode array of 20 interdigitated electrode fingers 10 μm in width spaced 15 μm apart are shown on COP being possible. The bonded chip was connected to via probes to an LCR meter with no noticeable electroosmotic bubbling at 50 mV AC (Figure 2.2B). An example of the direct immunoassay and electrode array from the underside of device is shown before and after silver enhancement (Figure 2.2C). The porous polymer monolith changes colors from white to a red-brown color after silver enhancement for positive test samples which corresponds with the expected color

change reported in optical detection studies.[69]
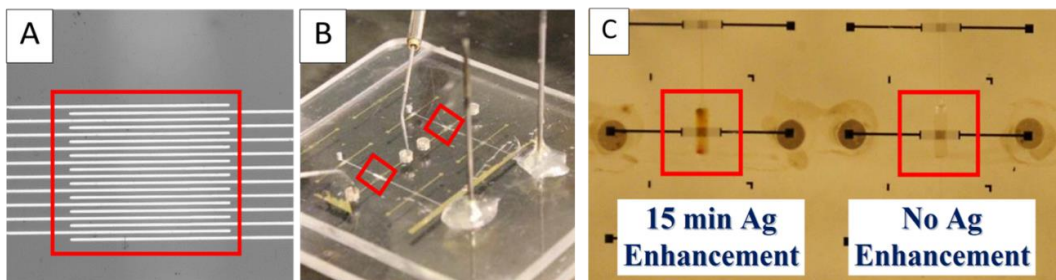
Figure 2.2: Interdigitated electrode array with 10 μm thick gold fingers spaced 15 μm apart on cyclic olefin polymer (COP) (A). A COP chip with inlet needle ports and probed, contact electrodes connected to an LCR meter is shown with a 100 μm tall and 350 μm wide channel in the sensing region (red square) are (B). The detection element is shown before and after silver enhancement for a positive sample (C).

2.4.2 Circuit Model and Performance

The equivalent circuit for the microchannel volume above the patterned IDA within the microfluidic channel is shown before[30] and after[70] the *in situ* formation of the porous monolith element (Figure 2.3). The total volume probed by the generated electric field for impedance measurements is determined by the geometry of the interdigitated electrode array. At least 95% of the total current that passes between the electrodes travels within a height equivalent to the electrode width and electrode gap added together.[60] This means that for an array of 10 μm wide gold electrodes spaced 40 μm apart, as tested in Figure 2.4, 95% of the current passes through the 50 μm directly above the electrode array. Thus, by increasing the electrode gap or electrode finger width a greater volume can be probed with the electric field limited only by the microchannel height.

For an open microchannel the contributions to the impedance of the circuit include the double layer capacitance at the interface between the electrode array and

the fluid (C_{dl}), the resistance of the fluid (R_{sol}), and the dielectric capacitance between

the electrodes themselves which for the electrode geometries and frequencies

employed has negligible impact on the measured impedance (Figure 2.3). The

equivalent circuit model results in a system with two zeros and two poles. At low

frequencies the impedance is dominated by the electrode double layer capacitance

(C_{dl}), while the bulk buffer resistance (R_b) dominates at high frequencies. A pole/zero

pair is introduced at intermediate frequencies, with locations that are functions of all

system parameters such as solution resistance, electrode geometry, and channel

geometry.
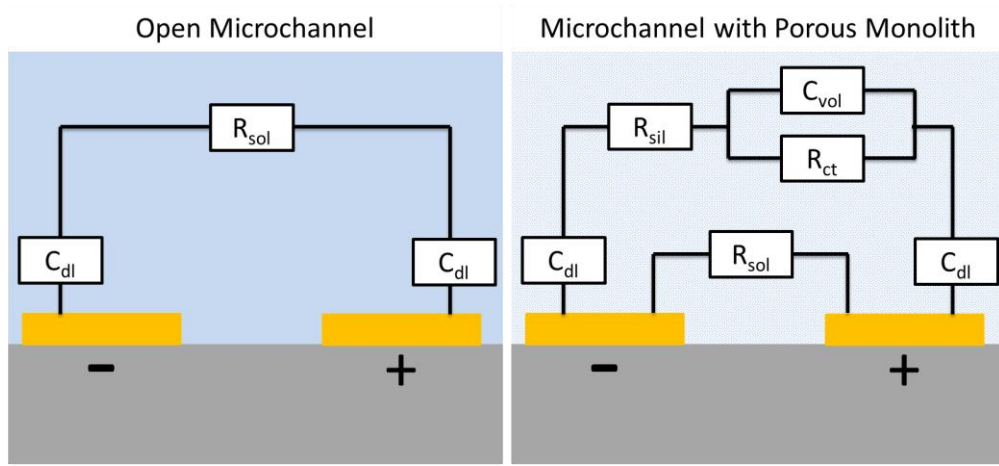
Figure 2.3: A diagram of the equivalent circuit between electrodes is shown before and after introduction of a porous volumetric detection element where C_{dl} is double layer capacitance, R_{sol} is solution resistivity, R_{sil} is the resistance of the silver clusters, Rct is the charge transfer resistance, and C_{vol} is the volumetric capacitance. The resulting model for impedance (Z) as a function of frequency (f) is also shown for the case of a channel containing a porous monolith.

The addition of a volumetric detection element and subsequent capture and

silver enhancement of AuIgG increases the complexity of the circuit. The porous

detection element adds a volumetric capacitance (C_{vol}) in parallel with a volumetric

charge transfer resistance (R_{ct}) in parallel with R_{sol} for the equivalent circuit (Figure

2.3). Measurements show the introduction of a non-conductive volumetric capture element into the microchannel results in an impedance increase. Instead of electrons passing through a highly conductive ionic solution that comprised 100% of the volume the electrons now must travel through the pores of the non-conductive monolith encountering a charge transfer resistance. In addition the non-conductive monolith element decreases the measured circuit capacitance by limiting double layer formation and thus increases capacitive reactance. This same trend is observed for polymer monoliths and silica bead beds. Thus the overall impedance magnitude increases and the phase

Figure 2.4: The impedance (A), capacitive reactance (B), and resistance (C) are shown at frequencies from 1 kHz to 250 kHz before and after silver enhancement of a silica bead bed capture element. The microchannel is 100 μm by 350 μm microchannel above an interdigitated electrode array consisting of 10 μm wide fingers spaced 40 μm apart.

angle increases with the addition of a non-conductive porous volumetric detection element.

The selective capture of (AuIgG) and formation of microscale silver aggregates within the porous detection element then further changes the measured volumetric impedance. The formed silver aggregates increase the volumetric capacitance (decrease in capacitive reactance) and decreases the volumetric charge transfer resistance causing the impedance to decreases as shown in Figure 2.4. Each silver particle formed has its own double layer capacitance that is a function of its total surface area causing an increase in volumetric capacitance and subsequent decrease in capacitive reactance. The conductive silver particles also decrease the volumetric resistance experienced by electrodes passing from the ionic solution into and out of the particle (R_{ct}). In addition electrons pass between the highly conductive silver clusters themselves (R_{sil}) lowering the impedance.. Because the number of silver aggregates formed is dependent on the number of captured AuIgGs the total decrease in impedance correlates with the target concentration. Thus as silver aggregates form the corner frequency associated with the intermediate pole is reduced, resulting in lower impedance at frequencies between the pole and the higher frequency zero. Because the density of silver aggregates is proportional to the concentration of captured AuNP-antibody conjugates, the total decrease in impedance at intermediate frequencies correlates with target concentration. This behavior can be seen in Figure 2.4, which presents experimental impedance curves generated during a sandwich immunoassay with 100 ng/mL target concentration. No noticeable change in impedance was caused by AuIgG capture alone during all experiments conducted.

While the above parameters help describe the circuit components, attempts to model the circuit were limited due to the lack of existing models. Fitting experimental

28

data to an equivalent circuit using Matlab was unsuccessful using different combinations of capacitors and resistors in series or parallel. A survey of the literature revealed the closest possible comparison for the circuit described here was in the field of supercapacitors that utilize an array of high surface area metal materials to generate high capacitance values.[70,71] To solve the problem of generating an equivalent circuit researchers in this field use a constant phase element (CPE) that includes a variable magnitude and a negative exponential variable in the place of a capacitance value alone. This constant phase element describes the interfacial dielectric properties of an imperfect capacitor in a volume and is placed in parallel with a volumetric charge transfer resistance that characterizes the DC conductivity to model supercapacitors.[70,71] While the physical meaning of the CPE is poorly understood it is commonly used in impedance spectroscopy to model experimental data more accurately than a simple parallel R-C circuit.[71] While using the constant phase element helped successfully fit experimental data to an equivalent circuit model the inability to use the model for comparison across devices and poor physical understanding limited its utility for this study.

2.4.3 Direct Assay Results

For a direct immunoassay using a polymer monolith the impedance change was defined as the change in impedance (Z_i-Z) divided by the initial impedance (Z_i) for the direct assay (Figure 2.5A). The optimal frequency for detection was 1 kHz as signal noise was too great at lower frequencies at the AC voltage used (50 mV) and the impedance change decreased as the higher frequencies. Using the control plus 3SD to define the noise floor the detection limit is 1.3 fM AuIgG after 15 min silver

29

enhancement with a 2 log dynamic range and 0.13 fM of AuIgG or $2.35*10^3$ particles after 30 min silver enhancement with a 3 log dynamic range. Trials with abnormal phase angles or abnormally high initial impedance values were discarded from analysis. For the control sample the impedance decreased due to non-specific silver aggregation on the electrodes and some non-specific aggregation within monolith. After 30 min silver enhancement the electrodes bridge for the 13 fM AuIgG resulting in an average impedance drop close to 100% and an average phase angle close to 0˚ and a statistically significant difference from the other tests samples. For each 40 nm diameter gold nanoparticle an estimated 167 anti-human IgG are attached giving an IgG detection limit of 2.14 fM. The molar detection limit is a 6 log improvement over a planar thermoplastic flow-through impedemetric immunosensor with unlabeled antibodies[30] and 10-fold improvement over silver enhanced non-microfluidic impedemetric immunoassays on silica[52] and glass[53] that require 1-2 h incubation steps and hand washing with distilled water. Measurement resolution was limited by variability between devices caused by *in situ* formation and functionalization of the UV cured polymer monolith[37] and minor variations in electrode geometry.
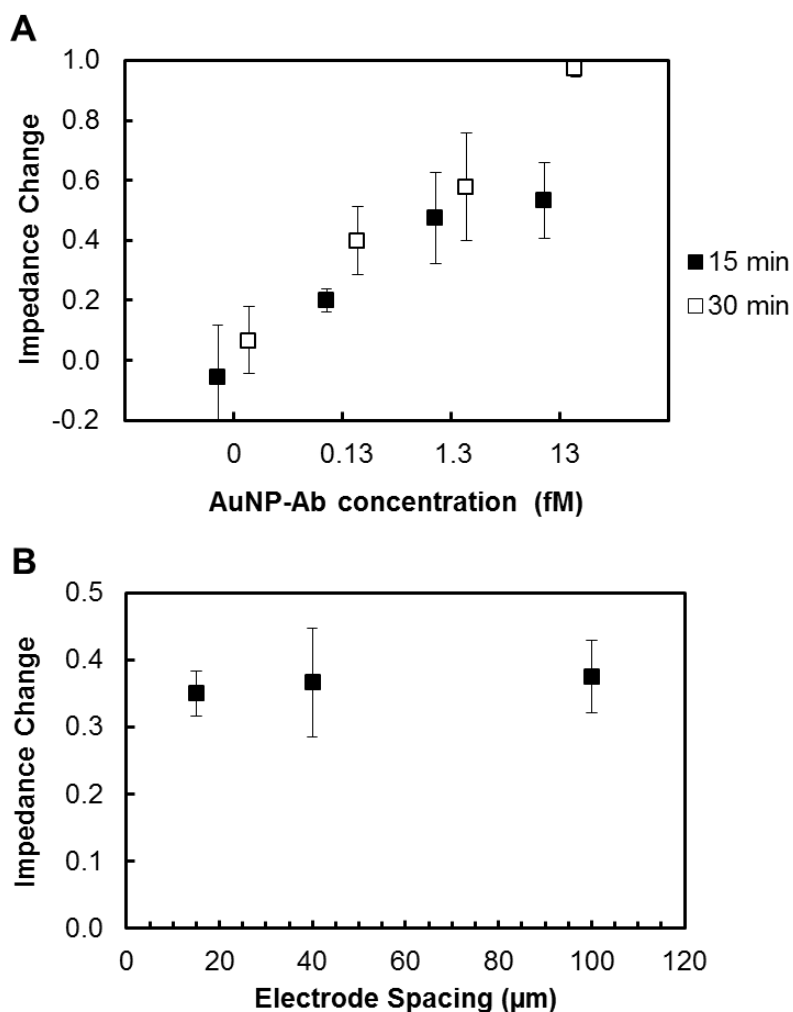
Figure 2.5: (A) Direct immunoassays were performed with different concentrations of AuIgG using an array of 10 μm wide electrodes spaced 10 μm apart, within channels containing porous polymer monolith detection elements. The impedance was measured at 1 kHz before (Z_i) and after (Z) 15 min and 30 min silver enhancement to determine the average impedance change (Z_i-Z/Z_i) for AuNP-IgG dilutions. For all tests n≥3 with error bars +/-1 SD. (B) A direct assay with 13 fM AuNP-IgG was performed with electrode arrays of 10 μm fingers spaced 15, 40, and 100 μm apart. The background corrected impedance change, control with no AuNP-IgG subtracted from variable, is shown at 1 kHz after 15 min silver enhancement. For all dilutions n≥3 except 40 μm control (n=2) with error bars +/- 1 SD.

Next the effect of electrode geometry on the sensor performance was

evaluated using interdigitated arrays of 10 μm wide electrodes spaced 15, 40, and 100

μm's apart below the porous polymer detection element (Figure 2.5B). Control

samples consisted of all assay steps except for AuIgG infusion while variable samples were infused with 13 fM AuIgG for 15 min before silver enhancement. The impedance change was calculated as described previously for all tests and averaged for each test condition. Then the impedance change of the control was defined as background and subtracted from the variable signal to compare across electrode configurations. The background corrected impedance change for each electrode configuration was approximately 0.4 with no statistically significant difference with different spacing (student's t-test, $p<0.05$). This is likely due to the fact that the relative volume containing silver enhanced AuIgG that affects the measured impedance is the same regardless of the probed channel volume. The results suggest that the volumetric impedance change is independent of electrode configuration as long as the microchannel is sufficiently tall enough to contain the generated electric field. A significant conclusion that may be drawn from these results is that the application of volumetric detection elements enables the use of low resolution electrodes that may be economically fabricated to achieve similar or better sensor performance than impedance based sensors employing planar detection elements which demand high resolution electrode arrays.

2.4.4 Sandwich Assay Results

A sandwich immunoassay was also conducted using both *ex situ* porous polymer monoliths and silica bead beds for volumetric detection elements. By employing *ex situ* elements functionalized with capture probes in a batch process the consistency across devices was improved. Characteristics such as capture probe density, porosity, and shape are uniform across test devices minimizing variation

between trials. The use of an *ex situ* elements integrated into a microfluidic channel is also more amenable to high-throughput manufacturing methods and can enable multiplex test creation by not relying on infusion of reagents through an *in situ* formed element for capture probe immobilization. The optimal frequency for impedance measurements was also 1 kHz for the sandwich assays. For the porous polymer monolith with an IDA of 10 μm fingers spaced 15 μm apart the detection limit was 1 ng/mL human IgG or $1.2 *10^8$ antibodies after 20 min silver enhancement using a noise floor of the control plus 3 SD (Figure 2.6B). Human IgG dilutions of 10 ng/mL and 100 ng/mL also exhibited a significantly greater impedance drop than control ($p < 0.05$). The molar detection limit of 6.54 fM IgG is 2 fold more sensitive than the best reported microfluidic assay using a planar PDMS/glass hybrid microfluidic device.[72] While the average impedance drop increased as human IgG concentration increased, none of the tested dilutions were significantly different from each other. Possible causes include non-specific silver aggregation after 20 min, variations in monolith integration position within the microchannel, electrode array geometry differences, and interactions between the polymer monolith and the negatively charged AuIgG causing non-specific capture. Non-specific silver aggregation may have been caused by light exposure, chloride ions in the PBS, variable infusion times, and the non-specific AuIgG capture.[49] Using light insensitive silver acetate, water rinses, multiple short silver enhancement periods, and a more uniform porous matrix could reduce the prevalence of non-specific aggregation to improve sensor performance.
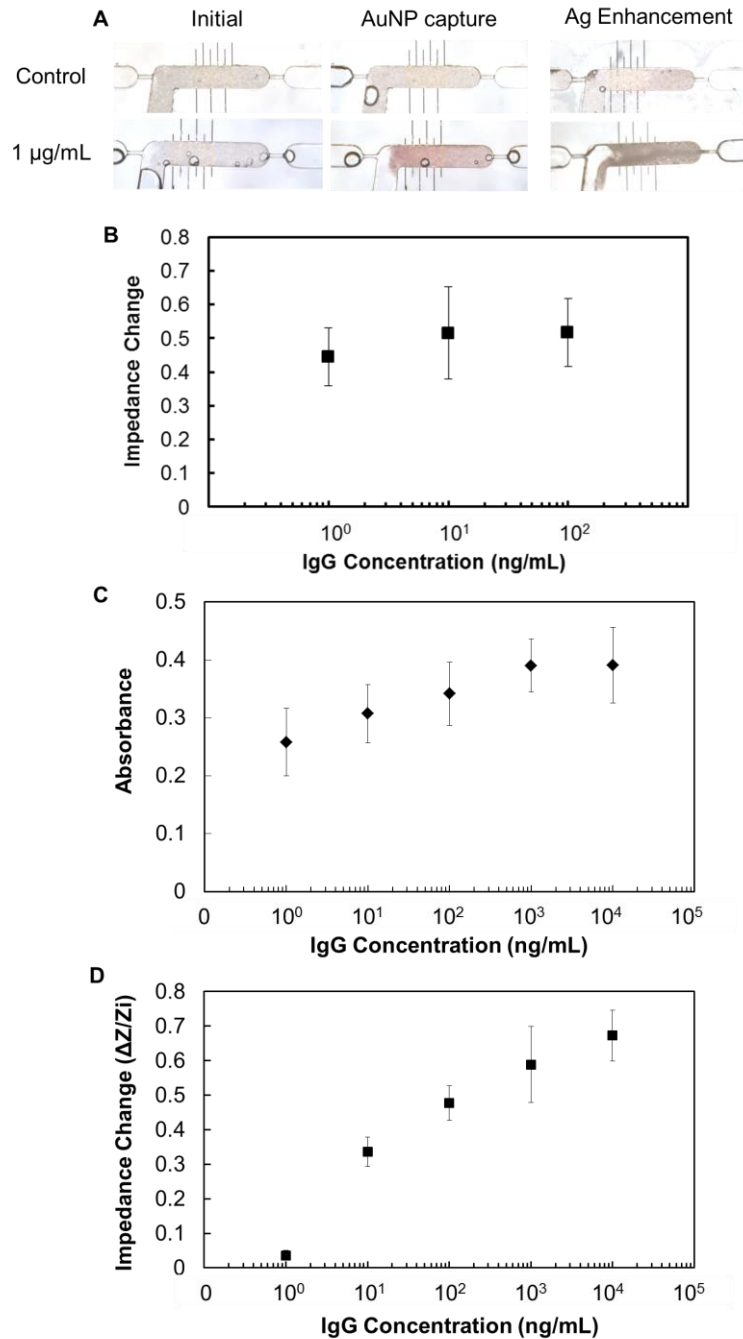
Figure 2.6: An example sandwich assay with silica beads is shown (A). A sandwich assay was completed using polymer monolith (B) with 15 µm electrode gaps and a silica bead bed (D) with 100 µm electrode gaps. The impedance was measured at 1 kHz before (Z_i) and after (Z) 15 min silver enhancement to determine the average impedance change (Z_i-Z/Z_i) for IgG dilutions. For all tests $n \geq 3$ with error bars +/- 1 SD except n=2 for 100 ng/mL (A) and 10 µg/mL (B) dilutions. The absorbance for the silica bead based assay was also measured for comparison (C).

To address these concerns a sandwich immunoassay was completed using a packed bed of functionalized 20 μm silica microspheres, HEPES buffer to minimize charge interactions between AuIgG and the detection element surface, and silver acetate enhancement solution (Figure 2.6A). The electrode array consisted of six 10 μm fingers spaced 100 μm apart in the microchannel. Measuring the optical absorbance alone the detection limit was 100 ng/mL with a 3 log dynamic range (Figure 2.6C) with relatively low measurement resolution. Measuring the impedance change after 15 min silver enhancement, the detection limit was 10 ng/mL or $1.2*10^9$ antibodies with a 4 log dynamic range and greater measurement resolution than previous experiments (Figure 2.6D). While the detection limit was higher the silver enhancement time was decreased to 15 min and the gold nanoparticle size was reduced from 60 nm to 40 nm to prevent electrode bridging thus minimizing the potential to detect low IgG concentrations.[33] When compared to similar planar based microfluidic assays (Figure 2.7) with respect to detection limit and total assay time both results the volumetric detection elements demonstrate superior performance. When compared to a bead bed detection element based conductance immunoassay that utilizes glass and PDMS and 20 micron electrodes[72] the detection limit is less with an additional 40 minutes of assay time. The wide dynamic range and relatively high measurement resolution suggests the potential for quantitation using a

volumetric impedance assay.
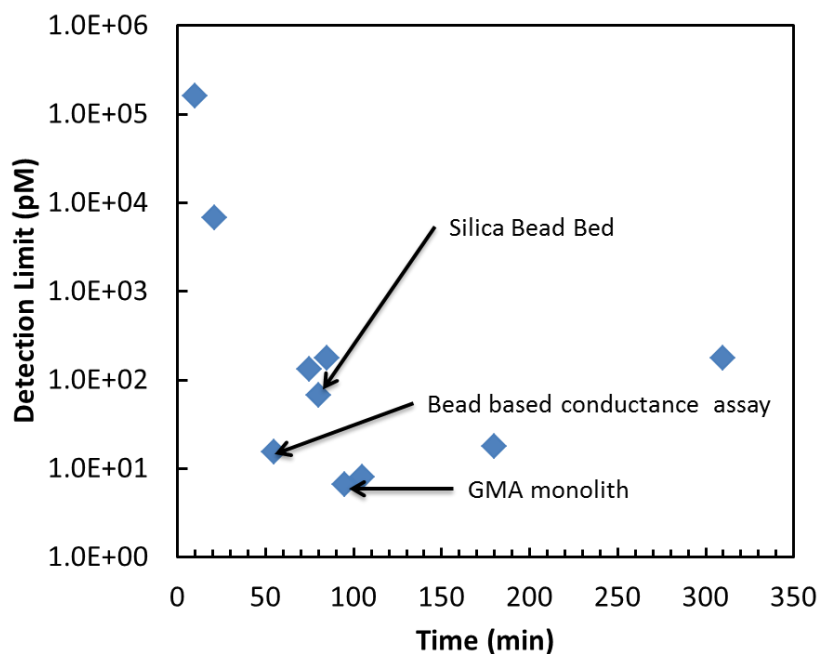
Figure 2.7: A comparison of detection limit vs. total assay completion time for sandwich immunoassays using electrically based sensing with IDA. All data points are for planar devices[30,52–55,73,74] with exception of a bead based conductance assay with 20 μm electrode resolution[72] and the results for GMA monolith and silica bead bed studies generated within this study.

There are many practical considerations when using silver enhancement in the assay design to achieve optimal detection performance. While light insensitive silver acetate was used for most of the experiments shown commercial silver enhancement solutions employ light sensitive silver nitrate that require careful storage before use. In addition the use of a distilled water rinsing step to remove ions that cause non-specific silver formation can improve test performance. The longer the silver enhancement time the greater the total exposed microsphere surface area and the decrease in the measured impedance. However as the silver microspheres grow indefinitely the electrodes eventually bridge reducing the phase angle to 0 degrees

and impedance to hundreds of ohms regardless of AC voltage frequency as the circuit becomes dependent on the silver concentration alone.[52] While the experimental design could be used to create a conductometric assay based on the time required to bridge the electrodes, this approach would require significantly longer incubation times. In addition the longer the silver enhancement time the greater the likelihood of non-specific silver aggregate formation increasing the signal noise. Finally the gold electrodes themselves act as silver aggregate formation sources causing a decrease in volumetric impedance that increases with longer silver incubation times. Further work is needed to optimize silver enhancement assay conditions, buffer conditions, gold nanoparticle size, and electrode configuration to optimize sensing performance.

With respect to electrode resolution moving from resolution on the order of 0.1-1 μm's, needed for planar devices, to 10-100 μm's, used in the demonstrated devices, to achieve comparable sensor performance can lower fabrication costs. If using a photolithographic process a less expensive mask can be used and a lower cost UV light source for electrode patterning. However moving from a photolithography process to a direct printing process can achieve 50% savings for electrode deposition while increasing througput.[75] For typical high throughput reel to reel processing direct inkjet printing can produce electrode resolution of >50 μm with a throughput of 50 m^2/hr, screen printing can produce >100 μm resolution with throughput of 100 m^2/hr, and flexography printing can achieve >50 μm resolution with throughput of 50,000 m^2/hr.[76] Each of these methods can be employed depending on the substrate, electrode material, and throughput desired to develop low-cost electrodes for microfluidic impedemetric sensors.

2.5 Conclusions

The presented thermoplastic device demonstrates a novel flow-through volumetric impedance immunosensor based on silver amplification of AuIgG within porous volumetric detection elements. The introduction of a porous volumetric element and subsequent silver enhancement of captured AuIgG decreased the capacitive reactance and resistance of the probed volume. For a direct assay, a detection limit of 0.13 fM 40 nm AuIgG was achieved after 30 min silver enhancement. For a sandwich assay, a detection limit of 1 ng/mL IgG was demonstrated after 20 min silver enhancement using 60 nm gold nanoparticle labeled secondary antibodies, and a detection limit of 10 ng/mL IgG was shown using 40 nm gold nanoparticles and a 15 min silver enhancement step. Both assays are relatively rapid (~75 min) compared to conventional planar immunoassays (2~3 h), and provide improved detection limits comparable to existing assays employing silver enhancement that utilize planar antigen capture surfaces. While demonstrated here using polymer monoliths and packed silica bead columns, the technique may be adapted for use with other porous volumetric detection elements customized for specific assays. The electrode resolution required and materials used are amenable to implementation in a low cost, disposable, manufacturable, and portable format requiring only a low-frequency ohmmeter for measurement, offering strong potential for POC tests including environmental monitoring and medical diagnostics.

Chapter 3: Optical Detection Enhancement in Porous Volumetric Microfluidic Capture Elements using Refractive Index Matching Fluids

3.1 Summary

This chapter presents a series of experiments completed through combined efforts with Dr. Annie Lu, Dr. Omid Rahmanian, and Mr. Luke Peterken and is adapted from an article in the journal *Analyst*. Dr. Lu contributed by conducting all fluorescent experiments using polymer monoliths within glass capillaries presented (Figures 3.3. and 3.4). Mr. Peterken contributed by conducting experiments to demonstrate the optimal aqueous sucrose solution for a silica bead packed bed (Figure 3.5) and aided in experiments to demonstrate a direct immunoassay (Figure 3.6). Dr. Rahmanian aided in experiments to demonstrate a direct immunoassay (Figure 3.6) and contributed to the editing of the journal manuscript.

In this chapter the use of porous volumetric detection elements in optical microfluidic sensors is demonstrated to achieve sensitvive and rapid sample analysis. Porous volumetric detection elements are advantageous compared to planar detection elements due to higher reaction site density and decreased diffusion lengths that can reduce detection limits and total assay time. However a mismatch in refractive indices between the capture matrix and fluid within the porous interstices results in scattering of incident, reflected, or emitted light, significantly reducing the signal for optical detection. Here we demonstrate that perfusion of an index-matching fluid within a porous matrix minimizes scattering, thus enhancing optical signal by enabling the

entire capture element volume to be probed. Signal enhancement is demonstrated for both fluorescence and absorbance detection, using porous polymer monoliths in a silica capillary and packed beds of glass beads within thermoplastic microchannels, respectively. Fluorescence signal was improved by a factor of 3.5X when measuring emission from a fluorescent compound attached directly to the polymer monolith, and up to 2.6X for a rapid 10 min direct immunoassay. When combining index matching with a silver enhancement step, a detection limit of 0.1 ng/mL human IgG and a 5 log dynamic range was achieved. The demonstrated technique provides a simple method for enhancing optical sensitivity for a wide range of assays, enabling the full benefits of porous detection elements in miniaturized analytical systems to be realized.

3.2 Introduction

Due to its flexibility, low infrastructure requirements, and potential for high sensitivity measurements, optical detection is a preferred sensing modality for many point of care (POC) diagnostic assays.[4] Interactions between incident photons and target analytes may be probed using a wide variety of optical sensing mechanisms including absorbance, colorimetric, fluorescence, interferometric, or spectroscopic detection. Optical detection is nearly ubiquitous for rapid POC molecular diagnostic tests, an area that is presently dominated by lateral flow assays.[77,78] In these tests, sample migrating through a porous substrate by capillary action binds with colored or fluorescent antibody-functionalized microparticles. Downstream capture of these antigen-specific particles by secondary probes results in selective particle accumulation, allowing qualitative analysis by direct optical observation, or semi-quantitative readout using a calibrated colorimetric or fluorescence reader. To

improve on the performance of lateral flow tests, microfluidic technology has been widely explored for the development of next-generation POC assays.[78] By taking advantage of various functionalization routes to anchor proteins, peptides, nucleic acids, or other assay-specific capture probes to the internal surfaces of microchannels, microfluidic technology offers great potential to realize improved assay throughput, reduce sample requirements, and enhance multiplexing capabilities. The surface-to-volume ratio scales favorably in microfluidic systems, such that smaller channels reduce the total sample volume required to deliver a fixed number of target molecules to capture probes anchored on the channel surface. However, the use of planar capture surfaces imposes a basic limitation on assay performance, since each channel wall may be functionalized with, at most, a single monolayer of probes. As a result, assay sensitivity and dynamic range are both constrained by the geometry of the capture surface.

As an alternative to planar capture surfaces, porous flow-through capture zones have been explored as an approach to realizing volumetric detection elements in microfluidic systems, allowing reaction site density to be greatly enhanced.[40,36] By minimizing pore dimensions for a given application, this approach offers the further benefit of reducing the characteristic diffusive length scales associated with interactions between target molecules in solution and molecular probes attached to the porous matrix surface, thereby enhancing assay speed. For optical detection, however, light scattering by micrometer-scale pores within a volumetric capture matrix presents an inherent constraint that can severely degrade sensor performance. Variations in the dielectric constant between the porous matrix and fluid within the

open pores result in strong coupling with incident light of wavelengths on the same order as the characteristic pore dimensions, leading to scattering of photons passing through the matrix.[45] Light scattering due to multiple changes in refractive index (n) significantly decreases optical transparency, with a concomitant reduction in sensitivity for measurements based on optical absorbance of target molecules or complexes within the detection zone. For fluorescence assays, transmission of photons associated with fluorophore excitation and emission can be reduced, similarly constraining measurement sensitivity. In general, regardless of the optical detection method, higher scattering results in a reduction of the probed volume, and thus a reduction in assay sensitivity.

Here we demonstrate the use of index-matching fluids to enhance optical performance in porous microfluidic capture elements. By infusing a fluid with the same refractive index as the porous medium itself, optical gradients within the detection volume may be reduced or eliminated, thereby minimizing light scattering and facilitating true volumetric detection within the functionalized porous sensor element. Fluorescence signal enhancement is demonstrated using porous polymer monoliths, with proof of concept shown by enhancing fluorescence signal of glutaraldehyde attached to the monolith, and biomolecular detection demonstrated through a direct fluorescence immunoassay with up to 2.6X signal amplification. Application of the index-matching technique is further demonstrated for an absorbance-based immunoassay with silver enhancement of gold nanoparticle labelled IgG (AuIgG), using a silica bead packed bed with an ordered porous structure in a thermoplastic microfluidic chip. For the absorbance based direct assay,

42

a detection limit of 0.1 ng/mL was achieved, with linear dynamic range of at least 5 logs, and up to two orders of magnitude higher sensitivity than related thermoplastic planar microfluidic immunosensors.[38]

3.3 Methods and Materials

3.3.1 Materials.

Glycidal methacrylate (GMA), hydrochloric acid (HCl), cyclohexanol, sodium hydrosulfide, citric acid, sodium citrate, sulfuric acid, 2,2-dimethoxy-2-Phenylacetophenone (DMPA), sodium phosphate dibasic, phosphate buffer saline (PBS), fluorescein isothiocyanate (FITC) labelled rabbit IgG, glutaraldehyde, bovine serum albumin (BSA), human IgG, (3-Aminopropyl) triethoxysilane (APTES), cyclohexane, sucrose, tris buffer, and hydroquinone were purchased from Sigma-Aldrich (St. Louis, MO). Ethoxylated trimethylolpropane triacrylate (SR454) is purchased from Sartomer (Warrington, PA). Bis(sulfosuccinimidyl) suberate (BS3), goat anti-rabbit IgG, and N-(γ-maleimidobutyryloxy) sulfosuccinimidyl ester (GMBS) were purchased from Thermo Fisher Scientific Inc. (Rockford, IL). Silver enhancement solution and 5 nm gold nanoparticle tagged anti-human IgG were purchased from Cytodiagnostics (Burlington, ON). Silica beads (20 μm diameter) were purchased from Corpuscular, Inc. (Cold Spring, NY). Silver acetate was purchased from Carolina Biological Supply Co. (Burlington, NC). Microfluidic fittings were purchased from IDEX Health & Science (Oak Harbor, WA) and needle tubing was purchased from Hamilton Syringe (Reno, NV). Capillary tubing with 360 μm O.D. and 250 μm I.D. was purchased from Polymicro Technologies (Phoenix, AZ).

3.3.2 Capillary Monolith Immunoassay with Fluorescence Readout.

GMA monoliths were formed in a silica capillary using a previously developed procedure.[40] After conditioning the capillary with 0.1 M HCl, a pre-monolith solution consisting of GMA (16%w/w), ethoxylated trimethylolpropane triacrylate (SR454) (24% w/w), cyclohexanol (50% w/w), methanol (10% w/w) was created. Next the photoinitiator 2,2-dimethoxy-2-phenylacetophenone (DMPA) was added at a ratio of 1:100 w/w with respect to the combined weight of the GMA and SR454. The combined solution was infused into the capillary masked with aluminum foil, and exposed to UV light with an incident power of 22.0 mW/cm^2 for 10 min. After UV-exposure the monolith section was rinsed with methanol and 20% methanol (v/v) aqueous solution and incubated with 2 M sodium hydrosulfide in a methanol-0.1 M aqueous sodium phosphate dibasic (20:80, v/v) for 2 h to transform epoxide groups to thiol groups. Remaining epoxide groups were hydrolyzed by overnight incubation at 65 ˚C with 0.5M sulfuric acid before rinsing with deionized water and ethanol. Finally 2 mM GMBS in ethanol was infused for 1 h followed by PBS rinsing to create amine-reactive NHS ester groups.

Initial fluorescence enhancement was demonstrated by infusing aqueous solutions of glutaraldehyde, an autofluorescent organic compound, through the monolith for direct attachment to the reactive monolith surface. This was followed by rinsing with deionized water for 5 min at 1 µL/min and infusion of GMA monomer for 5 min at 1 µL/min for refractive index matching. Next a direct assay was completed with the experimental setup shown in Figure 3.1.

44
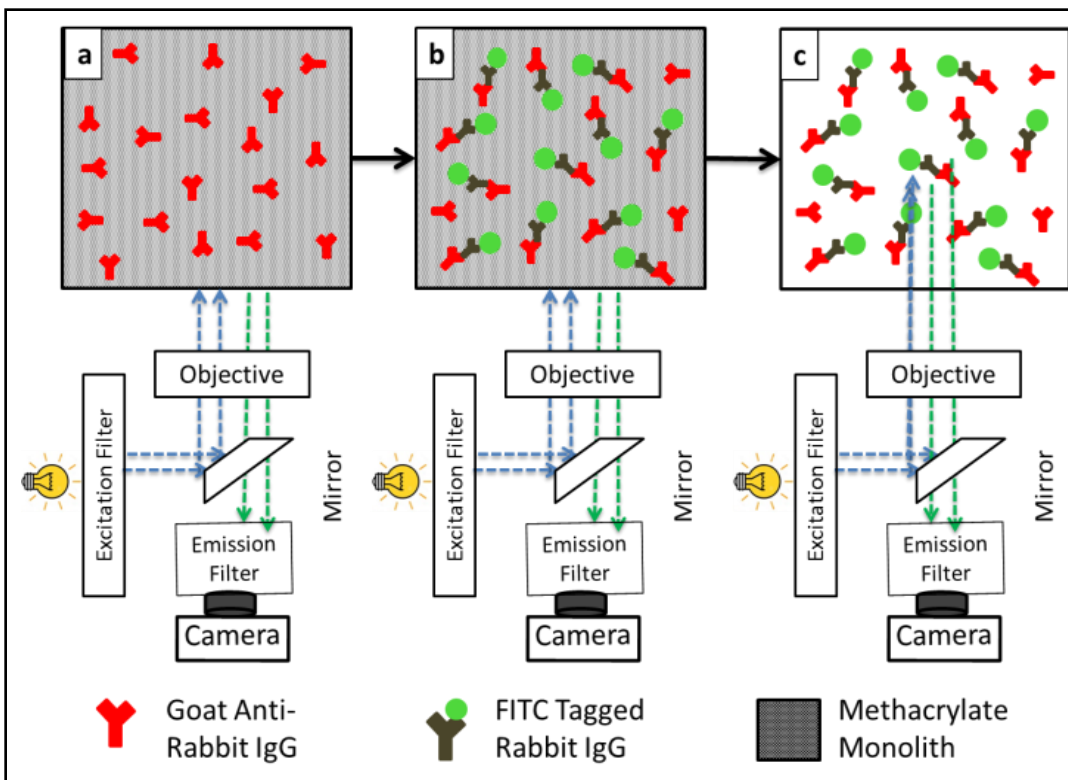
Figure 3.1: Experimental process for fluorescence based direct assay. The methacrylate monolith is covalently functionalized with goat anti-rabbit IgG (a) followed by infusion of FITC tagged rabbit IgG resulting in immobilization (b). Next GMA (n=1.45) was infused to enhance the fluorescence signal (c).

First 50 μg/mL goat anti-rabbit IgG in phosphate buffered saline (PBS) was infused for 1 h matching at 1 μL/min to react primary amines with exposed NHS ester groups on the GMBS treated monolith surface, followed by infusion of 2 mg/mL bovine serum albumin (BSA) in PBS matching at 1 μL/min for 15 min to block remaining reactive sites. This was followed by infusion of fluorescein isothiocyanate (FITC) labelled rabbit IgG at 2 μL/min for 5 min at concentrations of 0.1, 1.0, or 10 ng/mL. In each case, 2 mg/mL BSA in PBS was included with the immunoglobulins to serve as a dynamic blocking agent. Following IgG introduction, the monolith was rinsed with deionized water for 5 min at 1 μL/min, and GMA monomer was infused through the monolith for 5 min at 1 μL/min for index

matching. Imaging was performed using a B-2E/C filter cube (465-495 nm excitation, 515-555 nm emission) equipped on a TE-2000-S inverted epifluorescence microscope (Nikon, Melville, NY) with a CoolSnap HQ2 8-bit CCD camera (Roper Scientific, Tucson, AZ). An excitation wavelength within the range of 465–495 nm was selected using a B-2E/C blue filter (Nikon). Images were acquired continuously during water infusion and index-matching solution infusion. A region of interest 500 μm after the monolith beginning approximately 1 mm long and 150 μm tall was selected over the monolith section for before and after analysis using NIS elements software (Nikon).

3.3.3 Packed Silica Bead Immunoassay with Absorbance Readout.

Thermoplastic plates for fabrication were made with Zeonor 1020R cyclic olefin polymer (COP) resin (Zeon Chemicals, Louisville, KY) using a hot press (AutoFour/15, Carver, Inc., Wabash, IN). COP chips were cut to the desired size before channels and fluidic access ports were milled with a 3-axis desktop CNC milling machine (MDX-650, Roland DGA, Irvine, CA) and sonicated to remove debris. Channels were 150 μm deep and 300 μm wide in the sensing region with 40 μm deep and 50 μm wide regions which served as weirs to facilitate bead packing. The milled side and unmilled mating side were washed with methanol, isopropanol, and deionized water before N_2 drying and overnight degassing at 75 ˚C. The device was then solvent bonded with cyclohexane using an established procedure.[79,80] Briefly, the channel side was exposed to cyclohexane at 30 ˚C for 7.5 min before manual alignment and pressing with the mating side. The multilayer chip was then pressed at 1.38 MPa for 1 min at room temperature to complete the bonding.

Silica beads in a 5% wt. aqueous solution were functionalized with amine groups based on a previously reported method.[67] The beads were washed in piranha solution for 1 h before rinsing three times with deionized water and ethanol. Amine groups were introduced by incubating the beads in a solution of 5% (3-aminopropyl) triethoxysilane (APTES), 5% deionized water, and 90% ethanol (v/v) under agitation for 1 h at room temperature and washed 3 times with ethanol and PBS. Human IgG was attached to the beads using BS3, a homobifunctional amine-reactive crosslinker, by combining 900 μL of human IgG serially diluted in PBS, 100 μL of bead solution, and 35 μL of 7.19 mM BS3 in deionized water and incubating 30 min under agitation at room temperature. Control beads were functionalized by substituting human IgG with 2 mg/mL BSA in PBS. The reaction was quenched by adding 100 μL of 1 M tris buffer before agitating for 15 min at room temperature. The resulting mixture was washed 3 times with PBS and suspended in 2 mg/mL BSA in PBS overnight at 4 °C.

Functionalized beads were packed into a microfluidic device using vacuum through the side access channel into the restricted sensing region using a syringe and needle in the fluidic outlet port. Fluidic interfaces for off chip syringe pumps were created by inserting needle tubing segments into the access ports following a previously reported method[66] after the packed bed was formed. Fluidic fittings were attached to the needles and tests were conducted immediately.

3.3.4 Silver Enhancement.

To prepare a device for silver enhancement, 2 mg/mL BSA in PBS was infused for 15 min at 2 μL/min to prevent non-specific protein binding. Next, a splitter valve attached to the side channel was closed to ensure flow through the packed bed. Gold

47

nanoparticle anti-human IgG conjugate solution was diluted 1:50 in 2 mg/mL BSA in PBS and infused for 15 min at 2 μL/min followed by rinsing with 2 mg/mL BSA in PBS for 10 min at 2 μL/min. Silver enhancement solution was prepared using a two part mixture[68] chosen due to its stability under light exposure, consisting of 0.5 mg silver acetate in 5 mL deionized water and 1.25 mg hydroquinone in citrate buffer at pH 3.8. Deionized water was infused for 5 min followed by a 5 min infusion with silver enhancement solution combined in an off chip junction and a 5 min rinse with deionized water at 2 μL/min for each solution. Finally an aqueous index matching solution of 68% sucrose (w/w) was infused for 5 min at 3 μL/min. The experimental setup is shown in Figure 3.2.
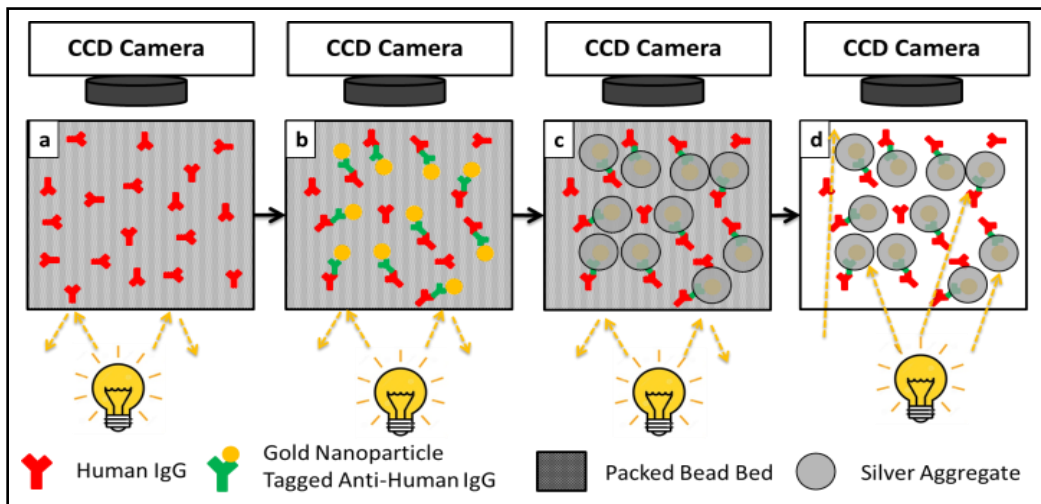
Figure 3.2: Experimental process for direct immunoassay using transmittance based detection. (a) A packed bed of silica beads with human IgG is (b) infused with anti-human IgG attached to gold nanoparticles (AuNP) that are (c) silver enhanced to create large aggregates prior to (d) introduction of index matching sucrose solution to render the volumetric matrix transparent for optical absorbance measurements.

Images of the chip before and after silver enhancement and after sucrose infusion were captured using an AZ 100 Multizoom microscope (Nikon) with diascopic lighting (see Figure 3.2). Illumination was provided by a halogen lamp

without filtering. Images were analyzed using NIS elements software. The region of interest (ROI) used to determine the intensity of the packed bed was taken from the middle third with respect to the x and y dimensions. In instances where bubbles were observed to form during sucrose infusion, regions containing bubbles were omitted from analysis. Transmittance (T) was determined as the average light intensity of the ROI divided by the intensity of a nearby featureless area, and the absorbance (A) was defined as 1-T.

3.4 Results and Discussion

3.4.1 Fluorescence Detection in Porous GMA Monoliths.

Selection of an appropriate index-matching fluid for microfluidic assays requires consideration of multiple factors such as optical clarity, viscosity, material compatibility, price, safety, and biocompatibility. For example, many commercially available organic solvents or oils with suitable refractive indices matched to the porous matrices explored in this work are either too viscous for infusion, not biocompatible, or incompatible with microfluidic device materials such as thermoplastics. Some aqueous index-matching solutions are compatible with thermoplastics and offer lower viscosity, but contain high salt concentrations that reduce antibody binding affinity and remove the target biomarker from the capture matrix. Alternate index-matching solutions are necessary for the technique to be useful for practical microfluidic assays.
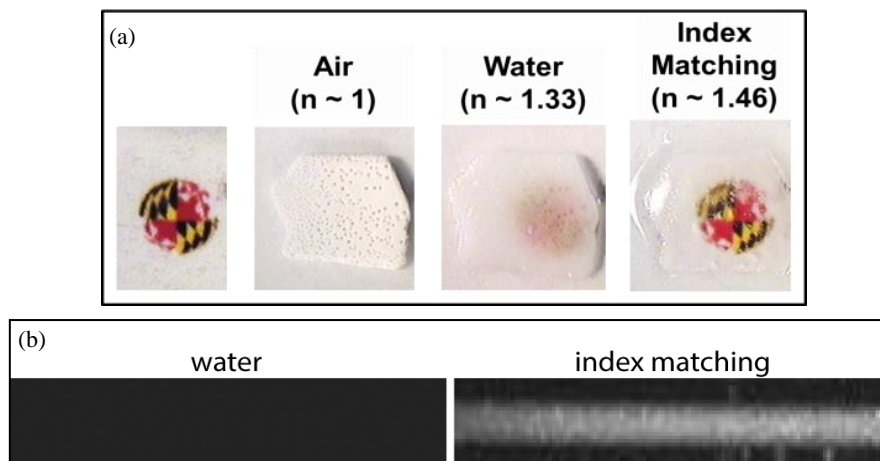
Figure 3.3: (a) An opaque monolith sheet in air (n~1) remains semi-opaque due to light scattering when water (n~1.33) is introduced. The addition of index-matching aqueous sucrose (n~1.46) significantly enhances transparency, revealing the image beneath. (b) Fluorescent intensity (I, arbitrary units) following water (I=758) and GMA monomer (I=2644) infusion through a glutaraldehyde functionalized monolith in a glass capillary.

The utility of index matching within a monolith structure to enhance optical transparency is shown by Figure 3.3a. The monolith is approximately 1 mm thick and the picture beneath is 2 mm in diameter. The monolith was photographed in air (n=1), after adding water (n=1.33), and after adding 68% aqueous sucrose solution w/w (n=1.46). As the refractive index of the solution approaches that of the monolith structure, light scattering within the monolith volume is reduced, facilitating visualization of the underlying image as the monolith transparency increases.

In the case of fluorescence detection, the porous medium used to support volumetric detection in this work consists of a GMA monolith anchored to the walls of a glass capillary. While detection of fluorescent species immobilized to the inner surface of silica capillaries[81,82] or species immobilized to fluorescent silica capillary surfaces[83] has been demonstrated, the use of a polymer monolith as a porous supporting scaffold can serve to increase volumetric probe density and reduce

diffusion length scale significantly compared with the use of open capillary systems. The monolith structure is a cylinder 250 μm in diameter and 1-2 mm long composed of spherical microglobules approximately 1 μm in diameter with an average pore size of 3~5 μm that create a tortuous flow path with high surface area for capturing probe immobilization.[40] Here we explored the use of GMA monomer (n=1.45) as a refractive-index-matching fluid. The monomer possesses a low viscosity similar to that of water, with a refractive index well matched with that of the monolith structure itself. Prior to introduction into the monolith, the GMA monomer was filtered to remove particles larger than 200 nm, but no additional chemical purification of the product was performed. Despite the relatively reactive nature of GMA, under the lighting conditions used in this work no observable polymerization was evident for GMA monomer in the absence of photoinitiator and crosslinker. We note that because GMA exhibits moderate toxicity, proper care should be taken during operation and disposal of devices employing this monomer for index matching. The GMA monomer was also found to result in some degree of quenching of the native autofluorescence of the monolith. Compared to the nominal fluorescence intensity measured for a non-functionalized monolith in air, the same monolith placed in water exhibited a 26% reduction in autofluorescence. In contrast, when placing the monolith in GMA a 48% reduction in fluorescence intensity was observed. To evaluate the impact of GMA index matching on the emitted optical signal for a fluorescent species, glutaraldehyde was immobilized through direct covalent bonding to amine groups on the monolith surface. Compared to the case of water, the fluorescence intensity of a glutaraldehyde

functionalized monolith perfused with GMA monomer was found to increase by a

factor of 3.5X, as seen in Figure 3.3b.

To investigate the use of GMA monomer as an index-matching fluid for

assays involving biomolecules, a direct immunoassay using FITC-tagged rabbit IgG

was explored. A polymer monolith within a silica capillary was functionalized with

goat anti-rabbit IgG before infusion with 0.1, 1.0, and 10 ng/mL of FITC-tagged IgG

in PBS. The fluorescence intensity during water infusion and during GMA infusion is

shown in Figure 3.4.
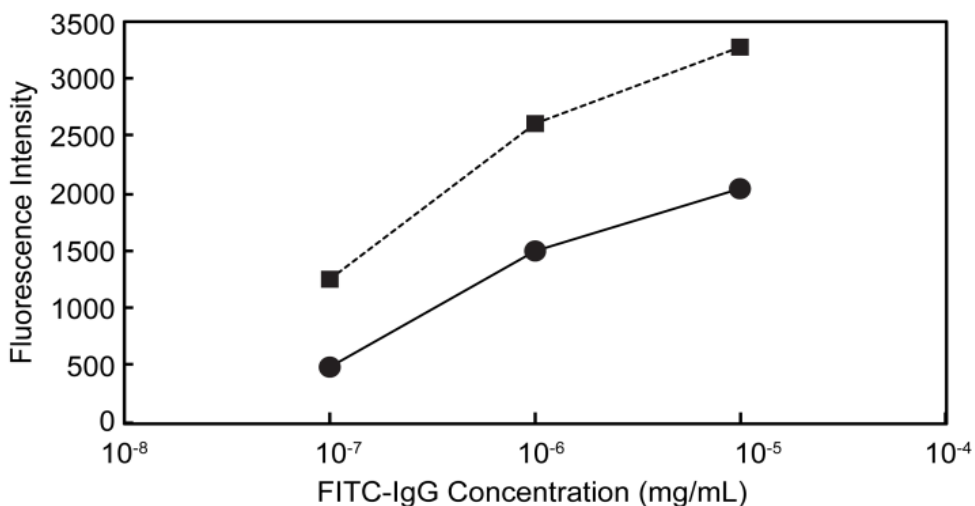
Figure 3.4: Direct assay with fluorescein isothiocyanate labelled antibodies before
and after infusion of GMA monomer through GMA-based monolith capture
element in a glass capillary.

As evident from this figure, index matching with the GMA monomer solution

significantly enhances the fluorescence signal, with increasing amplification as the

analyte concentration is reduced. A maximum signal enhancement factor of 2.6X was

observed at the lowest concentration of 0.1 ng/mL evaluated in this experiment. It is

also notable that the assay was completed within 10 min of sample introduction,

reflecting the ability of the porous matrix to encourage rapid probe-analyte

interactions.

Packed beds of microbeads are commonly used in both capillary and microfluidic systems as solid phase extraction media, stationary phases for chromatographic separations, and high area reactive surfaces. When combined with index matching, the use of packed beds as volumetric biodetection elements offers several advantages over *in situ* photopolymerized monoliths. Fabrication of a microfluidic packed bed is relatively straightforward, requiring only a simple weir structure to prepare the bed. Beads manufactured from a wide variety of materials with tailored sizes are readily available, allowing precise selection of bulk and surface properties as well as pore dimensions. Furthermore, conjugation of capture probes to the bead surface may be performed off-chip prior to bed packing, greatly simplifying the overall biosensor preparation process and providing a facile route to multiplexing.

Here we investigate the use of silica beads to prepare packed sensor beds in thermoplastic microfluidic chips, with aqueous sucrose solutions used as an inexpensive, low-viscosity, and biocompatible index-matching fluid. The refractive index of aqueous sucrose solutions varies nearly linearly with sucrose concentration, over a range of 1.33 for pure water to 1.50 for an 84% sucrose solution by weight.[84] Silica exhibits a refractive index of 1.46,[85] which is well matched by a sucrose concentration of 68%. To validate this assumption, the optimal index-matching solution was determined by infusing prepared aqueous sucrose solutions of various weight percentages through a packed bed of 20 μm diameter silica beads while measuring transmittance of light through the bed. As shown in Figure 3.5c, a maximum transmittance of 96.8% was observed during infusion of 68% sucrose

solution, as anticipated. In addition the transmittance magnitude is relatively insensitive for aqueous sucrose concentrations between 56% (n~1.43) to 74% (n~1.48). Sucrose concentrations greater than 74% were found to be too viscous for reliable perfusion through the porous silica bead beds.
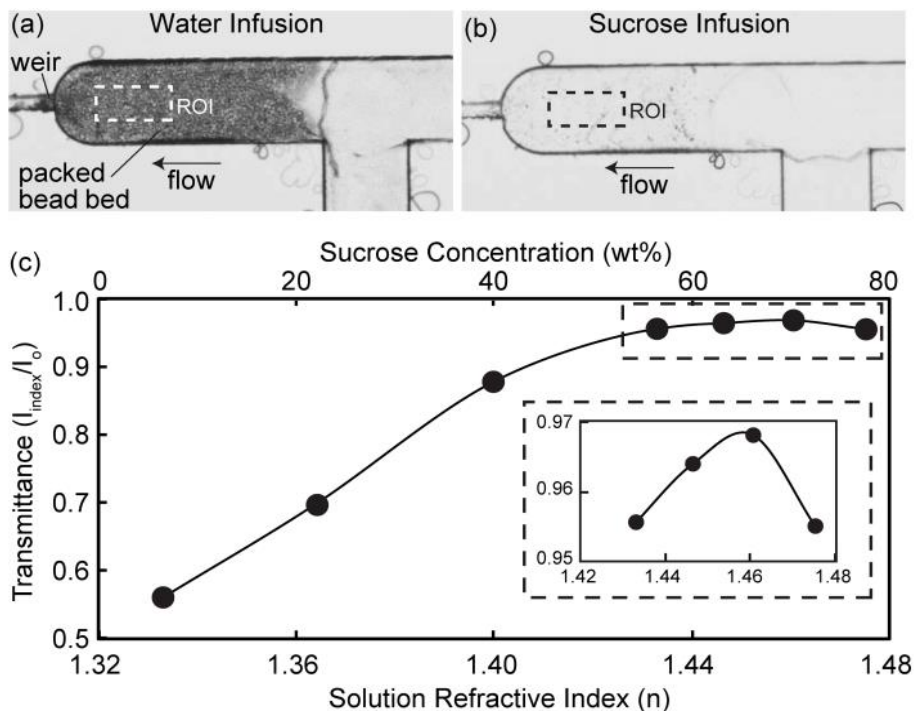
Figure 3.5: Images of a packed silica bead bed infused with (a) water and (b) 68% sucrose in water (n=1.46). (c) Measured light transmittance with varying sucrose concentration. Transmittance is defined as the ratio of average transmitted intensity of a region of interest (ROI) of the packed bed after sucrose infusion (I_{index}) to the background intensity (Io) of a nearby region of the chip.

Attempts to complete an absorbance based assay with a GMA polymer monolith in a thermoplastic microchannel were unsuccessful due to inherent material properties. The GMA monolith itself was minimally transparent (~20%) when infused index matching solutions compared to the silica bead bed tested likely due to a smaller pore size and less consistent structure. In addition, the hydrophobic polymer monolith caused significant pressure build-up during aqueous sucrose infusion

compared to hydrophilic porous silica bead beds that made consistent infusion conditions difficult. Finally the hydrophobic monolith also caused non-specific capture of negatively charged gold nanoparticles in the buffers used increasing signal noise and increasing the feasible detection limit. Thus a silica based volumetric element was employed for the direct assay described later.

Because direct observation of absorbance changes resulting from the accumulation of native target biomolecules results in high detection limits, some form of optical enhancement is typically employed for absorbance-based assay readout, for example through the application of enzymatic amplification or use of a secondary probe capable of generating a high absorbance signal. Here we combine index matching in a packed microfluidic silica bead bed with the latter method, together with a silver amplification step to further increase assay sensitivity. Silver amplification was chosen due to the ease of handling, inexpensive reagents, robustness, and high sensitivity.[49] In this method, micrometer-scale silver clusters are grown on AuNP labelled biomolecular probes, resulting in large absorbance signals for the resulting assay. This approach has been previously demonstrated for enhanced optical detection of many biological targets including nucleic acids[69,86] as well as antibodies[33,87–89] and other proteins[90,91] with detection relying on colorimetric readers,[86] scanometric methods,[69,87,91] CCD cameras,[88,89] or direct visual inspection[92] with the naked eye to detect silver aggregate formation.[49] However, many optical immunoassays employing silver enhancement are presently limited in their utility for near-patient use. Existing assays use planar capture surfaces that limit the number of biomarker recognition events and detector sensitivity. To overcome this limitation

long incubation times and repeated hand pipetting are required that are not conducive to rapid diagnostics. Many studies use glass and silicon based devices that can be fragile and are often too expensive for disposable near-patient tests, or silicone elastomers that are not economically viable for high throughput production.[2,10,12,13] For thermoplastic substrates, challenging immobilization chemistries limit the capture probe density and thus assay sensitivity.[33,38] Thus we propose combining off chip functionalized elements into a low-cost thermoplastic device that is adaptable to large-scale manufacturing.

The combination of index matching and silver amplification in a volumetric silica bead bed was investigated using a thermoplastic COP chip design. The fabricated chip contains a contains a weir for trapping silica beads injected through a side port to create a packed bed with a nominal pore size of ~5 μm, together with an inlet port for the introduction of AuNP-labelled sample, silver amplification solutions, and index-matching fluid (Figure 3.6a). Using this platform, a dilution study was performed to evaluate the impact of index matching on assay sensitivity and dynamic range. The bead bed is initially white before infusion of AuNP anti-human IgG conjugates. Beads conjugated with relatively high human IgG concentrations (>10 μg/mL) will become pink to the naked eye after AuNP conjugate binding while those with less human IgG will remain white even though AuNP conjugates are captured. Following introduction of silver enhancement solution the white bead bed begins to darken to a reddish-brown as silver aggregates form on the captured AuNP's. No removal of silver aggregates due to shear forces generated by the relatively high viscosity of the aqueous sucrose solution was observed at the flow rates used. As seen

in Figure 3.6a, increasing concentration of immobilized human IgG leads to the

formation of more silver aggregates in the bead bed that absorb the incident light.
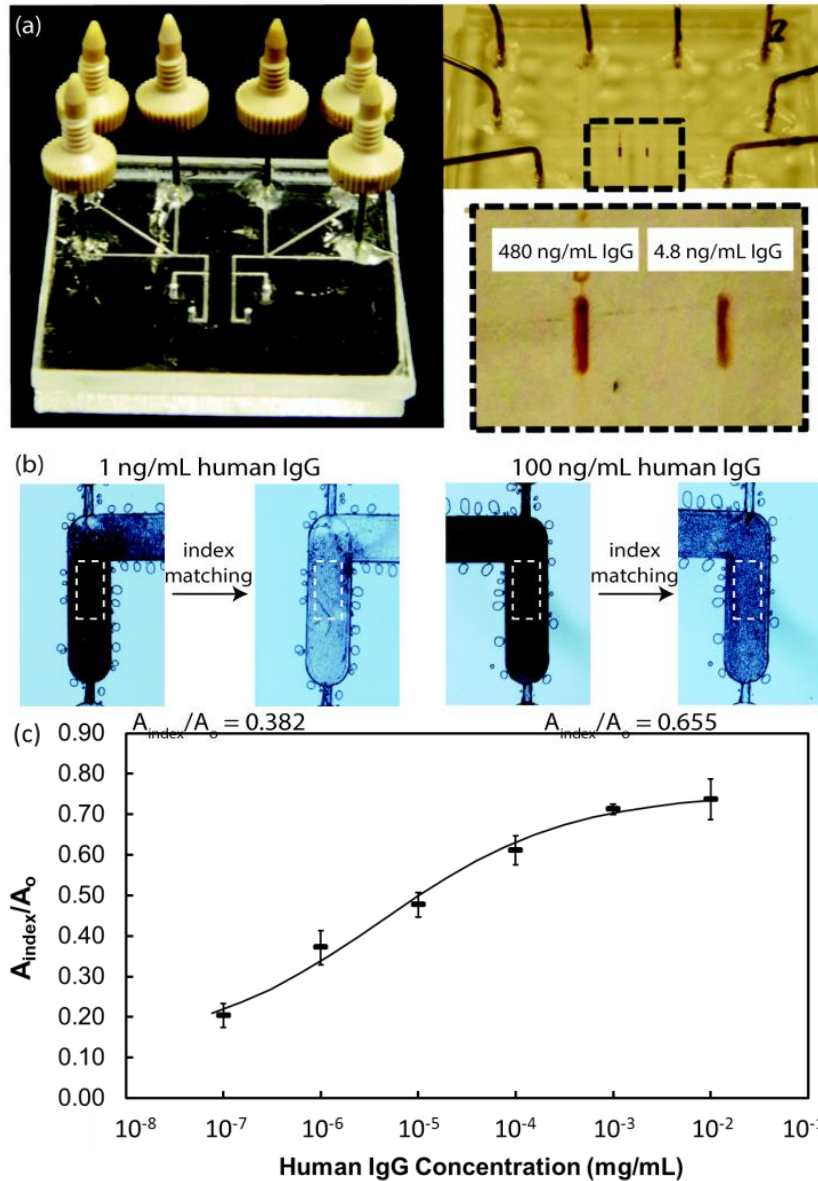
Figure 3.6: (a) Microfluidic chip containing silica bead detection zones, with the bead beds alternately functionalized with either 480 ng/mL or 4.8 ng/mL of human IgG. The magnified image of the packed bed is shown after selective capture of AuNP anti-human IgG conjugates and subsequent silver amplification. (b) Absorbance was measured for the regions of interest shown (dashed boxes) after silver enhancement and water rinse, and after infusion with a 68% sucrose solution for index matching. (c) Relative absorbance for a silver-enhanced direct immunoassay following infusion of index matching solution in a microfluidic silica bead.

Example images of the porous detection matrix following silver amplification and index matching are shown in Figure 3.6b for two representative concentrations of human IgG bound to the beads. The relative absorbance, defined as the ratio of absorbance after index matching (A_{index}) to the absorbance after silver enhancement and water rinsing but before index matching (A_o), was analyzed to evaluate detection limit, dynamic range, and sensitivity. By employing relative absorbance as the assay output, the impact of variations in lighting conditions caused by fluctuations in ambient lighting and lamp output, as well as variations in chip geometry that might impact optical performance, were minimized to reduce signal variance across test devices.

Relative absorbance measurements from a dilution study covering a range of human IgG concentration from 0.1 ng/mL to 10 μg/mL are presented in Figure 3.6c. From inspection of this data, and defining a conservative noise floor as the average relative absorbance of the negative control monolith plus 3 standard deviations ($3\sigma =$ 0.189), a minimum detectable signal of 0.1 ng/mL (0.65 pM) was achieved. For comparison, the minimum detectable human IgG concentration before and after silver enhancement with water infusion was 10 μg/mL, revealing the significant benefits of index matching to assay sensitivity. At high analyte concentrations, signal saturation is observed above 1 μg/mL (student's t test with $p < 0.05$) thus defining an overall dynamic range of 5 logs (0.1 ng/mL to 1 μg/mL). Each dilution tested within this range is well differentiated from each other ($p < 0.05$) demonstrating good control of signal noise. The data is consistent with a sigmoidal dependence between optical signal and antibody concentration, as expected based on Langmuir binding

kinetics.[93,94] Compared with microfluidic immunoassays requiring significantly longer assay times on the order of 60-90 min,[38,51] the demonstrated molar detection limit is approximately 1-2 logs lower than these previously reported devices employing planar capture surfaces. The improved sensitivity and large dynamic range confirm the utility of index matching as a strategy for enhancing the performance of optical detection from three dimensional porous matrices. Furthermore, we note that for the particular device implementation explored in this work, the low material and fabrication costs associated with thermoplastic microfluidics offers potential for disposable diagnostics that may be used at the POC, while the robustness of the optical detection scheme supports integration with a portable photodetector or camera, LED excitation source, and lightweight power supply for use in remote and resource-limited environments.

Several potential practical limitations of the technique should be noted. For any particular application, issues relating to the viscosity and biocompatibility of candidate index matching fluids must be carefully considered, and the case of sensors involving biomolecular interactions, the potential degradation of these interactions by the index matching fluid must also be evaluated. The addition of index matching as a required step increases assay complexity, while the Integration of porous microfluidic capture elements can present its own challenges compared to simpler planar surface modification methods. Regardless, the significant improvement in assay performance that can be achieved using the reported method, in terms of both assay sensitivity and time, offers a promising solution for a wide variety of demanding microfluidic sensing applications.

3.5 Conclusions

This work demonstrates refractive index matching as a flexible method for enhancing optical signals in microfluidic assays with porous volumetric detection elements. The technique facilitates the advantages of porous sensing elements such as rapid assay times and sensitive volumetric analyte capture while minimizing the effects of light scattering that compromise optical measurement sensitivity. Fluorescent signal was amplified by a factor of 3.5X for attached fluorescent glutaraldehyde and 2.6-1.6X for a direct immunoassay that took ~10 min to complete. For an absorbance-based direct assay using silver enhancement, the detection limit was 0.1 ng/mL with a 5 log dynamic range and a total time of 45 min to complete. These results demonstrate volumetric optical detection techniques that could be adapted for detection of numerous biomarkers such as bacteria, viruses, proteins, toxins, or nucleic acids. Future development applied to simple, low cost POC devices for environmental monitoring or medical diagnostic tests can improve detection limits, allow quantification of dilute targets, and reduce total assay times compared to existing technology.

Chapter 4: Flow-through Microfluidic Immunosensors Employing *ex situ* Functionalized Silica Monoliths as Optical Detection Elements

4.1 Summary

In this chapter, a sensitive and rapid absorbance based immunosensor that utilizes *ex situ* funtionalized porous silica monoliths as volumetric optical detection elements is demonstrated. The porous monolith structure facilitates high capture probe density and short diffusion length scales, enabling sensitive and rapid assays. Silica monoliths, synthesized and functionalized with immunocapture probes off-chip before integration into a sealed thermoplastic microfluidic device, serve to capture target antigens during perfusion through the porous structure. Gold nanoparticle immunoconjugates (AuIgGs) combined with silver enhancement is used to create microscale silver clusters, followed by perfusion of an aqeuous sucrose solution to limit light scattering and enhance optical signal. Using this approach, detection limts as low as 1 ng/mL are achieved for a sandwich assay, with a dynamic range of at least 5 logs. The results confirm that *ex situ* functionalized porous silica monoliths can enable sensitive and rapid detection of target antigens, with potential for multiplexed detection using thermoplastic microfluidic assays with low variance between devices.

4.2 Introduction

Optical detection is a preferred sensing modality for many diagnostic assays for its flexibility, low infrastructure requirements, and potential for high sensitivity measurements.[4] Optical detection is nearly ubiquitous for lateral flow assays that

dominate commercial rapid point of care (POC) diagnostic tests.[77,78] For these tests

the biological sample travels by capillary action across the substrate and biomarkers

within the solution bind to colored or fluorescent antibody-functionalized

nanoparticles such as colloidal gold or colored latex beads.[48] These complexes are

then captured downstream by immobilized capture probes and accumulate facilitating

qualitative analysis by direct optical observation or semi-quantitative analysis using a

calibrated colorimetric or fluorescent reader.[48] To improve on lateral flow test

performance, microfluidic technology has been widely explored for next-generation

diagnostic assay development.[78,37] Microfluidic assays can improve multiple common

assay steps including reagent consumption reduction, higher throughput, integration

of multiple assay steps, automation, and multiplexing capabilities.[37,95,96] An important

consideration in microfluidic assay design is the material used to construct the device

and its microchannels. Many studies use glass and silicon based devices that are

fragile and often too expensive for diagnostic assays or silicone elastomers that are

not economically viable for high throughput production.[2,10,12,13] In contrast

thermoplastics such as polymethylmethacrylate (PMMA), polycarbonate (PC),

polystyrene (PS) and cyclic olefin polymers (COP) are attractive because they are

inexpensive, robust, and scalable for industrial manufacturing by injection molding or

hot embossing.[10,12,13] Thus thermoplastic based LOC devices show the greatest

promise for robust, low-cost, diagnostic tests for a diverse array of biological

samples.[17]

 Most microfluidic assays employ various functionalization routes to anchor

proteins, peptides, nucleic acids, or other assay-specific capture probes to chemically

modified internal microchannel surfaces.[37] The high surface-to-volume ratio inherent

to these microfluidic channels reduces the total sample volume and/or incubation time

required to deliver a fixed biomarker concentration to capture probes anchored on the

channel surface. However, the use of planar microfluidic channel surfaces for

biomarker capture limits assay performance since each channel wall can be

functionalized with, at most, a single monolayer of probes. For thermoplastic

substrates specifically challenging immobilization chemistries limit the effective

capture probe density.[33,38] As a result, assay sensitivity and dynamic range are

constrained by both the geometry and available surface chemistry of the microfluidic

channel.

In contrast to planar capture surfaces, porous flow-through biomarker capture

elements can significantly increase reaction site density.[40,56] By optimizing porosity

and pore size the characteristic diffusive length scale between target biomarkers in

solution and capture probes attached to the porous matrix surface are reduced, thereby

enhancing assay speed and sensitivity. These porous elements can also improve assay

performance by introducing materials with surface chemistries enabling significantly

more efficient anchoring of biomolecular capture probes than typical thermoplastic

surfaces. A variety of macroporous materials have been explored as matrices for

selective biomarker capture in microfluidic systems including packed bead beds,

hydrogels, polymer monoliths, membranes, paper, and porous silicon.[37] However, a

limitation common to all of these materials when used for optical detection is that

light scattering within the volumetric capture matrix presents an inherent constraint

that diminishes sensor performance. Variations in dielectric constant between the

porous matrix and fluid within the open pores causes strong coupling with incident light, leading to scattering of photons passing through the matrix.[45] This light scattering can significantly decrease optical transparency, limiting the probed volume and reducing sensitivity for optically based assays. A further limitation is that many macroporous materials such polymer monoliths typically require *in situ* polymerization and functionalization. This constraint increases fabrication cost and complexity, particularly for the case of multiplexed devices employing multiple sensing elements with different capture probes, and creates the potential for excessive batch-to-batch variability.[44]

Here we demonstrate a microfluidic immunoassay with a simple optical readout that overcomes issues of light scattering and challenging *in situ* synthesis to achieve rapid and sensitive antigen detection. The platform employs off-chip functionalized silica monoliths integrated into thermoplastic microchannels as discrete porous detection elements. The rigid silica monoliths are synthesized in a polymer mold using a sol-gel chemistry[97] and then functionalized *ex situ* with antibody capture probes using silane chemistry. The silica monolith segments are the inserted into a solvent softened thermoplastic microchannel to physically embed the outer layer into the channel walls to efficiently seal the monoliths to force fluid flow through the pores during assay operation.[64] The immunoassay consists of selective capture of AuIgG followed by silver enhancement to create micron scale silver clusters. An aqueous sucrose solution with the same refractive index as the silica is then infused through the monolith to eliminate index gradients and thereby enhance optical signal using a technique previously demonstrated within a microfluidic packed

silica bead column.[56] Using this approach, both absorbance and reflectance based measurements were investigated for optical assay readout. For the case of absorbance measurements, detection limits between 1-10 ng/mL for a direct assay and 10 ng/mL for a sandwich assay were achieved, with linear response over a dynamic range of up to 5 logs. For a reflectance based sandwich immunoassay, a detection limit of 1 ng/mL was realized over a 5 log dynamic range after index matching.

4.3 Methods and Materials

4.3.1 Materials.

Tetramethoxysilane (TMOS), polyethylene glycol (PEG) (10,000 MW), ethanol, acetic acid, phosphoric acid, ammonium hydroxide, citric acid, sodium hydrosulfide, sulfuric acid, sodium citrate, sodium phosphate dibasic, phosphate buffer saline (PBS), fluorescein isothiocyanate (FITC) labelled rabbit IgG, glutaraldehyde, bovine serum albumin (BSA), 4-(2-hydroxyethyl)-1-piperazineethanesulfonic acid (HEPES), human IgG, (3-Glycidyloxypropyl)trimethoxysilane (GPTMS), Tween 20, sucrose, tris buffer, and hydroquinone were purchased from Sigma-Aldrich (St. Louis, MO). Decahydronaphthalene (decalin) and N-(γ-maleimidobutyryloxy) sulfosuccinimidyl ester (GMBS), anti-human rabbit IgG were purchased from Thermo Fisher Scientific (Rockford, IL). 5 nm gold nanoparticle tagged anti-human IgG and anti-rabbit IgG (AuIgG) were purchased from Cytodiagnostics (Burlington, ON). Silver acetate was purchased from Carolina Biological Supply Co. (Burlington, NC). Microfluidic fittings were purchased from IDEX Health & Science (Oak Harbor, WA) and needle tubing was purchased from Hamilton Syringe (Reno, NV). Capillary tubing with

360 μm O.D. and 250 μm I.D. was purchased from Polymicro Technologies (Phoenix, AZ).

4.3.2 Silica Monolith Preparation.

The procedure for preparation and reintegration of silica monoliths into thermoplastic microchannels described below was developed and optimized by Dr. Eric Kendall. Silica monoliths were formed in a poly(methyl methacrylate) (PMMA) (US Plastic, Lima, OH) mold using a procedure previously developed for discrete polymer monolith production.[97] The channel side of the mold was milled with a CNC machine 3-axis desktop CNC milling machine (MDX-650, Roland DGA, Irvine, CA) using an endmill with a 45 degree angled tip to a depth of 350 μm to create a negative mold feature with a trapezoidal cross section profile. The milled plaque was sonicated to remove debris and washed with methanol, isopropanol, and deionized water before drying with N_2 and degassing overnight under vacuum at 75 °C. The milled mold together with a flat PMMA capping layer were exposed to UV ozone treatment for 10 min using a (Novascan PSD-UV, Ames, IA) and pressed together at 75 °C at 2.07 MPa for 10 min using a hot press (AutoFour/15, Carver, Inc., Wabash, IN). Silica monolith precursor solution was prepared by stirring 20 mL of 0.01 M acetic acid in an ice bath for 5 min. Next 1.88 g of PEG was added and stirred for 10 min to fully dissolve before adding 9.28 g TMOS and stirring 30 min in the ice bath. The precursor solution was then introduced into the PMMA mold using capillary action. The channel ends were sealed and the mold was incubated at 40 °C in an oven for 48 h to complete the gelation process. The silica monoliths were then removed from the PMMA mold after removing the weakly-sealed capping layer and immersed in 0.01

M ammonium hydroxide overnight at 40 °C to complete solvent exchange. The monoliths were then rinsed three times with deionized water and dried at 120 °C overnight before being heated at 600 °C for 2 h to burn out the PEG, and cooled to 50 °C. The monoliths were then cut into 1.2 mm long segments, rinsed three times with ethanol, and then dried.

The silica monoliths segments were functionalized with capture probes as shown in Figure 4.1a. The monolith segments were then immersed in 5% GPTMS in toluene for 18 h, rinsed three times with toluene and ethanol each, and dried. Next the monoliths were immersed in 2 M sodium hydrosulfide in 20% methanol-80% 0.1 M aqueous phosphate dibasic adjusted to a pH of 8.15 with 2 M phosphoric acid for 4 h, rinsed three times with deionized water, and incubated in 0.5 M sulfuric acid overnight at 65 °C. The monoliths were then immersed in a 2 mM GMBS in ethanol for 4 h and rinsed three times with 1x PBS. For the direct assay either the monolith was incubated for 2 h in either serial dilutions of human IgG in 1x PBS ranging between 10 ng/mL to 10 µg/mL or 2 mg/mL BSA in 1x PBS (control) before incubating overnight in 2 mg/mL BSA in 1x PBS at 4 °C. For the sandwich assay all silica monoliths were incubated for 2 hours in 10 µg/mL human IgG in 1x PBS before overnight storage in 2 mg/mL BSA in 1x PBS at 4 °C.
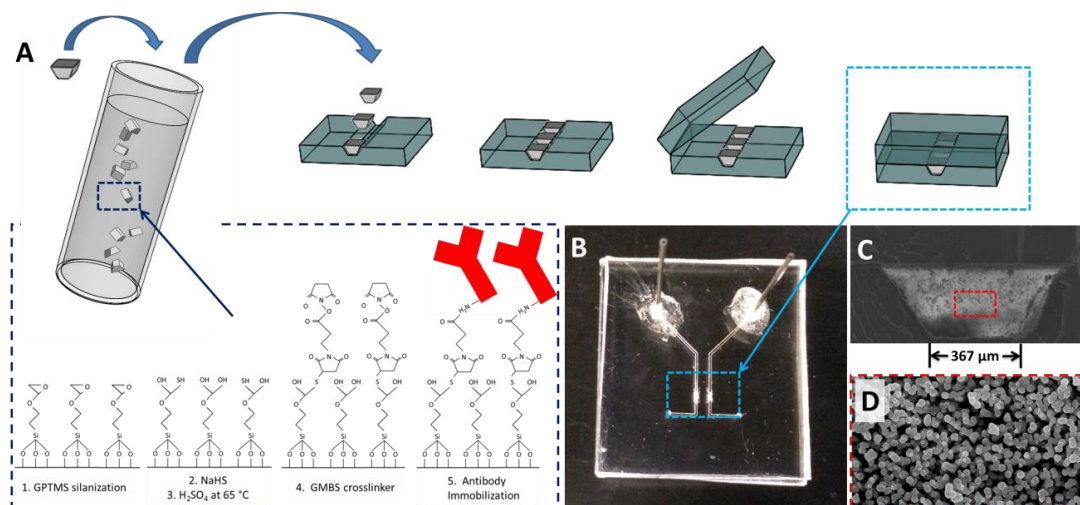
Figure 4.1: The fabrication of the microfluidic device is outlined here (A). Porous silica monolith segments created within a mold with a trapezoidal cross section are functionalized with antibodies using the surface chemistry shown. The functionalized inserts are then placed into an open microchannel with a trapezoidal cross section and sealed using solvent bonded cyclic olefin polymer (COP). A picture of the constructed microfluidic device is shown (B) with an SEM image of the detection zone cross section (C) demonstrating a fluidic seal with the channel walls. A close up SEM image of the porous silica monolith structure shows globules are 2 µm in diameter and an average pore size of approximately 2.5 µm (D). Dr. Eric Kendall provided the 3-D cartoons used in this figure.

4.3.3 Microfluidic Chip Preparation with Reintegrated Silica Monolith Segments.

Thermoplastic plates for immunoassay device fabrication were made with Zeonor 1020R cyclic olefin polymer (COP) resin (Zeon Chemicals, Louisville, KY) using a hot press (AutoFour/15). COP chips were cut to the desired size before channels and fluidic access ports were milled with a 3-axis desktop CNC milling machine (MDX-650) and sonicated to remove debris. Channels were 250 µm deep and 780 µm wide at the top and 380 µm wide at the base in the sensing region. The milled microchannel substrate and unmilled capping layer were washed with methanol, isopropanol, and deionized water before N_2 drying and overnight degassing at 75 ˚C. Individual silica monolith segments were then inserted into the device

68

before solvent bonding with decalin as shown in Figure 4.1a. Briefly, each side was exposed to 30% decalin in ethanol (v/v) for 5.25 min before dipping in ethanol and blow drying excess solvent with N_2 gas. Next the silica monolith segment was placed into the milled trapezoidal sensing region using a wetted paintbrush as described by Kendall et al.[64] The two COP surfaces were then placed together by hand and pressed at 1.38 MPa for 10 min at room temperature to complete the bonding. Fluidic interfaces for off chip syringe pumps were created by inserting needle tubing segments into the access ports following a previously reported method[66] and were stored at 4 °C until use. All devices were used within 24 h of bonding.

4.3.4 Direct Immunoassay Procedure.

Optimization of the buffer conditions and incubation times described in the section below was aided by Dr. Jin-Hee Han. Syringe pumps were connected to the microfluidic device at room temperature using capillary tubing connected to stainless steel tubing ports press fit into the inlet ports of the chip. First, 2 mg/mL BSA in 10 mM HEPES buffer with 140 mM NaCl was infused for 10 min at 2 μL/min as a static coating to minimize non-specific protein binding on the monolith surface and channel walls. Next, AuNP-labelled anti-human IgG solution was diluted 1:50 (v/v) in HEPES buffer containing 1% BSA and 0.05% Tween 20 and infused for 15 min at 2 μL/min, followed by rinsing with 2 mg/mL BSA in HEPES for 10 min at 2 μL/min to remove unbound sample. Silver enhancement solution was prepared using a two part mixture[68] chosen due to its stability under light exposure, consisting of 1.0 mg silver acetate in 5 mL deionized water and 2.5 mg hydroquinone in 5 mL citrate buffer at pH 3.8. Deionized water was infused for 5 min followed by a 5 min infusion

with silver enhancement solution combined in an off chip junction, and a 10 min rinse with deionized water at 2 μL/min for each solution. Finally an aqueous index matching solution of 68% sucrose (w/w) was infused for 5 min at 3 μL/min. The refractive index to the sucrose solution was ~1.46 which matches the refractive index of the porous silica monoliths.[56] The experimental setup is shown in Figure 4.2.
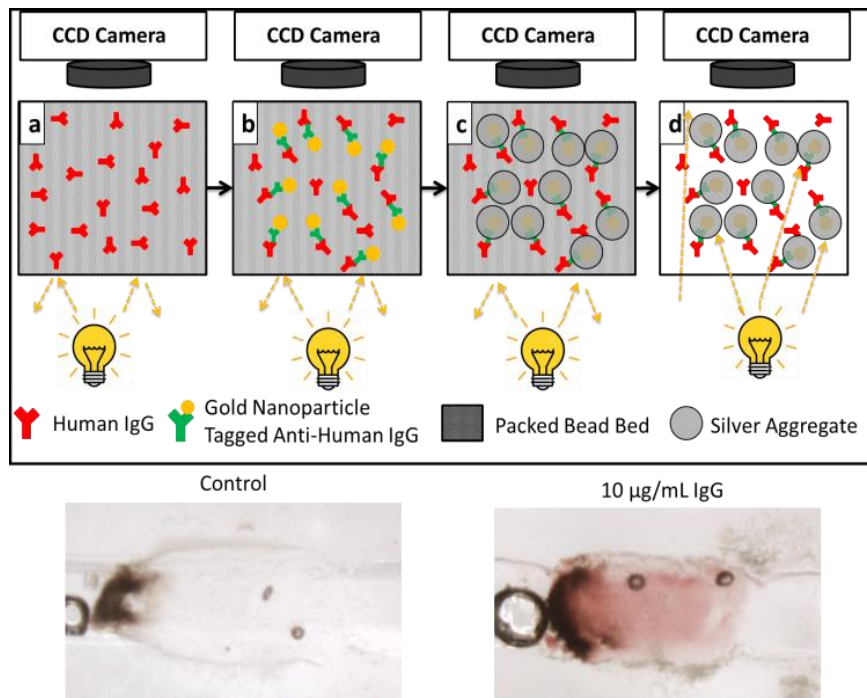
Figure 4.2: Direct immunoassay process using transmittance based detection. (a) A silica monolith with human IgG is (b) infused with anti-human IgG attached to gold nanoparticles (AuNP) that are (c) silver enhanced to create large aggregates prior to (d) introduction of index matching sucrose solution to render the volumetric matrix transparent for optical absorbance measurements. When the assay is complete a control test is white while a high concentration test results in a reddish-brown silica monolith due to silver enhancement.

4.3.5 Sandwich Immunoassay Procedure.

The device was treated similarly as the direct assay. After 10 min of infusion with 2 mg/mL BSA in HEPES buffer, rabbit IgG at concentrations from 1 ng/mL to 10 μg/mL in 1x PBS were infused for 15 min at 2 μL/min. This was

70

followed by 10 min infusion of 2 mg/mL BSA in HEPES buffer, 15 min of

AuNP anti-rabbit conjugate solution diluted 1:50 (v/v) in HEPES buffer

containing 1% BSA and 0.05% Tween 20, and 10 min 2 mg/mL BSA in HEPES

buffer at 2 µL/min. Silver enhancement was carried out as described previously

with 5 min deionized water rinsing, 5 min silver enhancement, and 10 min

deionized water rinsing. Finally a 68% aqueous sucrose solution (w/w) was

infused for 10 min at 1 µL/min through the device.

4.3.6 Image Analysis.

Images of the chips before and after each assay step were captured using a

color CCD camera (DFK 41AU02, The Imaging Source, Charlotte, NC). For

transmittance imaging, the chip was positioned on an AZ 100 Multizoom microscope

(Nikon) with diascopic lighting provided by a halogen lamp without filtering (Figure

4.2). Transmittance (T) was determined as the average light intensity of the ROI

divided by the intensity of a nearby featureless area, and the absorbance (A) was

defined as 1-T. Reflectance images were captured by illuminating the chips with a

150 W ring illuminator light source (Fiber-Lite 180 Illuminator, Dolan-Jenner

Industries, Boxborough, MA) attached to a stereoscope (S8 APO, Leica

Microsystems, Buffalo Grove, IL). Each chip was positioned with its lower surface 2

mm above a cleanroom cloth (Texwipe TechniCloth Nonwoven Dry Wiper, Fisher

Scientific, Pittsburgh, PA) which served to provide a uniform white background with

low specular reflection for imaging. Images were captured using the DFK color CCD

camera in an episcopic configuration.

For both transmission and reflection measurements, Images were analyzed using Image J software. The region of interest (ROI) used to determine the intensity of the silica monolith was 300 μm by 600 μm in area, and positioned approximately 200 μm downstream from the entrance into the silica monolith. This region of interest excludes the sloped sidewalls to ensure consistent optical measurements across samples. In instances where bubbles were observed to form during sucrose infusion, regions containing bubbles were omitted from analysis.

4.4 Results and discussion

4.4.1 Device Preparation.

Reproducible operation of the immunoassay requires that fluids flow through the porous silica monolith structure, rather than entering gaps between the monolith and microchannel sidewalls, since non-uniform flow profiles during any assay step can result in irreproducible optical signals. During the sol-gel curing process the silica monoliths were observed to shrink, resulting in final monolith elements that were approximately 70-65% the width and height of the original PMMA mold dimensions. Accordingly, the COP microchannels into which the monoliths were integrated were designed to be approximately 10% smaller than the final monoliths to ensure a tight seal.[64] By exposing the mating COP sides to the decalin/ethanol mixture, a solvent softened surface layer formed that under pressing filled the outer layers of the silica monolith creating a tight seal with the microchannel walls,   as shown in Figure 4.1c.[64] The sloped sidewalls served to encourage the monolith to settle into the channel after manual placement, and generate a normal force component during

sealing that ensured reliable bonding between the monolith and microchannel surfaces without gaps or cracks. The technique was attempted using monoliths with rectangular cross section, but this geometry was commonly found to either result in gaps between the channel sidewalls and the monolith, or fracture of the monolith due to stress concentrations during the sealing process. In contrast with *in situ* polymerization or packed bead bed methods used for volumetric capture element creation there is excellent anchoring of the silica monolith to the COP caused by interlocking of the materials.

There were many properties of the silica monolith inserts that had to be considered when fabricating the devices. The silica monoliths were somewhat brittle limiting the length to width ratio (L/W) of the inserted elements. For longer segments (L/W > 5), the monoliths often fractured during handling, while shorter segments (L/W < 0.25) would not align reliably. For consistent results, monoliths 1.2 mm long and 270 μm tall, with lower and upper widths of 380 μm and 780 μm, were used here. The brittle nature of the monoliths also resulted in small debris breaking off during the placement process that would become trapped in the solvent softened polymer during bonding. Similarly, because the channels are 10% smaller in cross-sectional dimensions than the monolith elements, the upper edges of the monoliths experience high forces during sealing that can lead to surface fracturing and the formation of debris. These debris appear as darkened regions surrounding the edges of the channel, but are fully encased in COP after bonding and thus do not affect the fluid flow.

4.4.2 Direct and Sandwich Immunoassay Using Absorbance Based Detection.

Optical absorbance detection was first explored based on the transmission of light from a source positioned on one side of the monolith to a detector located on the opposite side. Most absorbance based immunoassays utilize some form of amplification to enhance the optical signal, such as enzymatic amplification or the use of a secondary probe to increase the absorbance signal per binding event. To increase optical signal in the present work, a secondary gold nanoparticle probe was used in combination with a silver amplification step, followed by refractive index matching to minimize the detection limit and maximize dynamic range of the immunoassay. The silver amplification step utilizes stable, inexpensive reagents[49] to enhance optical detection as previously demonstrated in a variety of microfluidic immunoassays[33,87–89] using colorimetric readers,[86] scanometric methods,[69,87,91] CCD cameras,[88,89] or direct visual inspection with the naked eye[33] to detect silver aggregate formation[49]. Because most existing microfluidic assays employing silver enhancement are based on the use of planar capture surfaces, they require long incubation times to achieve low detection limits. The porous volumetric capture elements explored here, combined with index matching fluids to limit light scattering within the porous matrix, offer potential to achieve low detection limits with shorter incubation times by taking advantage of the high surface area and small diffusion length scale associated with the porous monolith structures.

A direct assay was first demonstrated to validate the performance of *ex situ* functionalized silica monoliths integrated into thermoplastic microchannels. Serial concentrations of human IgG or BSA (control) were covalently bound to the silica

monoliths *ex situ* and then integrated into a sealed microchannel. After device

fabrication, AuNP-conjugated anti-human IgG was infused and selectively captured

on the functionalized silica monolith surface. At high IgG concentrations (>10

μg/mL) the white silica monolith was observed to turn pink to the naked eye, while at

lower concentrations no change was observed. Next, optical signal from the captured

AuNP's was enhanced by silver amplification to create micrometer scale silver

aggregates that turn the monolith a reddish-brown color. Finally, aqueous sucrose

solution was infused to match the refractive index of the porous monolith, thus

amplifying optical signal by minimizing light scattering. No removal or displacement

of silver aggregates due to flow-induced shear forces during infusion of the viscous

aqueous sucrose was observed at the flow rates used in these experiments.

Example transmission based images of the porous silica monolith capture

region after each assay step including index matching are shown in Figure 4.3a. As

the concentration of immobilized human IgG increases, more AuNP's are captured

and thus more silver aggregates form. Thus as human IgG concentration increases the

detection region becomes darker due to absorption of the incident light. The ratio of

absorbance measured after index matching (A) to the initial absorbance after silver

amplification (A_o) was used to define the relative absorbance (A/A_o). The relative

absorbance of the control sample was defined as background and subtracted from the

relative absorbance at each concentration to compare performance across assays. By

employing background corrected relative absorbance the impact of variations in

lighting caused by changes in ambient lighting or lamp output and variations in chip

geometry were minimized to reduce signal variance across different trials.
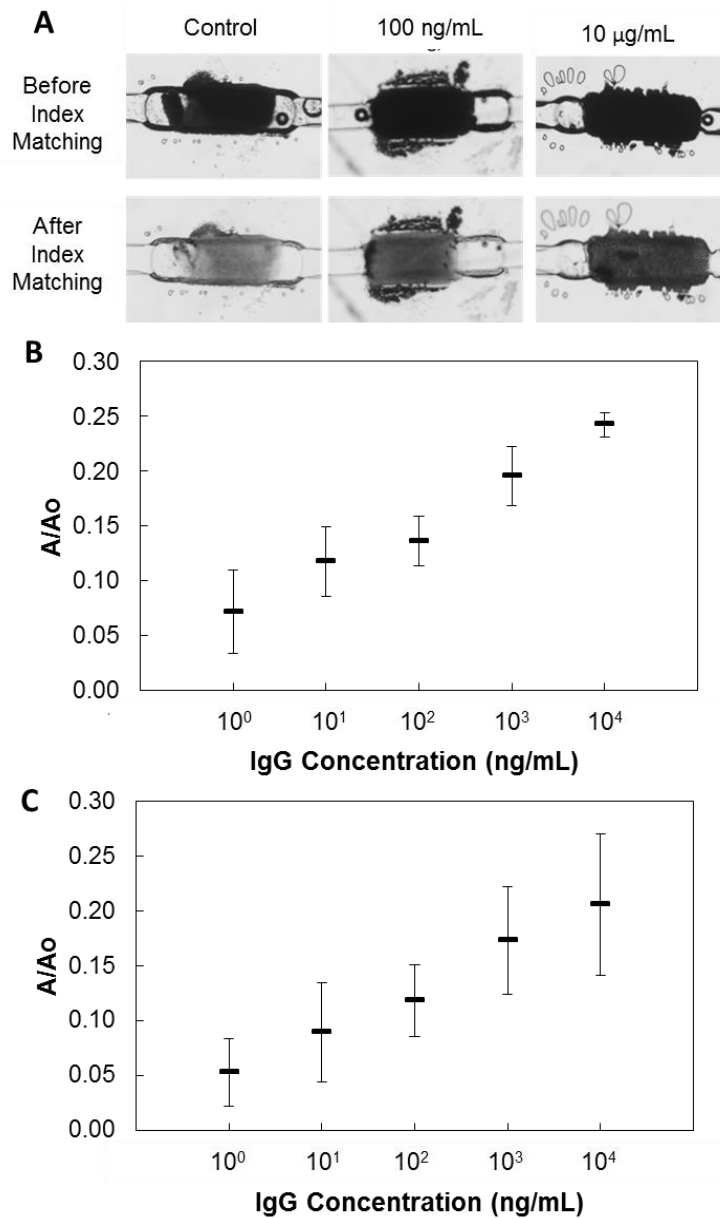
Figure 4.3: (A) Grayscale images of the silica monolith detection region are shown for a direct assay before and after index matching with different concentrations of IgG used during monolith functionalization. Background corrected relative absorbance (A/Ao) plots for (B) a direct immunoassay and (C) a sandwich immunoassay are presented for each concentration of human IgG and anti-human IgG, respectively. For each datum, $n \geq 3$ and error bars represent +/- 1 SD.

Relative absorbance measurements from the direct immunoassay covered a range of human IgG concentrations from 1 ng/mL to 10 µg/mL are presented in Figure 4.3b. From inspection of this data and defining the noise floor as control plus 3

76

standard deviations, a detection limit between 1-10 ng/mL was achieved. Using a student's t test with $p < 0.05$ the measurement resolution was approximately 2 logs with an overall dynamic range of 5 logs. These results verify that capture antibodies immobilized on the silica monolith surface prior to integration into the microfluidic device maintain their affinity to target IgG throughout the full set of chip fabrication steps.

Relative absorbance measurements from the sandwich immunoassay covered a range of anti-human IgG concentrations from 1 ng/mL to 10 µg/mL are presented in Figure 4.3c. As with the direct assay, a detection limit between 1-10 ng/mL was achieved, with an overall dynamic range of 5 logs. The detection limit is similar to the results of a previously-reported sandwich immunoassay using a planar functionalized thermoplastic surface requiring multiple pipetting steps and 60 min IgG and AuNP conjugate incubation steps to complete.[38] In comparison, the assay presented here requires 15 min to complete the IgG and AuNP conjugate incubation steps using a simple flow-through protocol that is readily amenable to automation.

For the case of transmission based detection, relatively low measurement resolution was observed, indicating a high level of variance in measured absorbance data. The light must travel in one direction through multiple interfaces between the silica monolith and COP surface before reaching the CCD camera causing variation in light transmission between devices. The lighting used was unfiltered white light from a diffuse source beneath the microfluidic device. Optimization of lighting using lenses to focus the light and increase the wavelength of the incident light could help minimize the light scattering. Additionally because light has to travel through the

entire monolith volume any variations in the monolith structure or small trapped air bubbles in the viscous sucrose solution will cause variance between samples. Methods to reduce bubble formation such as biocompatible surfactants could also help reduce variation.

4.4.3 Sandwich Immunoassay Using Reflectance Based Detection.

The sandwich assay was also evaluated using reflectance based imaging of the porous silica capture region. For POC applications, reflectance imaging offers several advantages over transmission imaging. Illumination and imaging are both done on the same side of the device minimizing the need for a custom optics set-up and facilitating the use of portable cell phone cameras for imaging and analysis. The optical path length examined can be increased up to 2x using reflectance based imaging to enhance sensitivity. Finally the effect of the volumetric capture element depth on variance between devices is reduced since the light will penetrate and reflect back at the same depth and at multiple angles independent of the element size to help average the optical signal. For the completed assay the measurement resolution was much lower for reflectance imaging compared to transmission imaging. In this case, images were captured after anti-human IgG infusion, AuIgG capture, silver enhancement, and index matching solution infusion as shown in Figure 4.4a. The intensity of the region of interest, imaged using an 8 bit color CCD camera, was determined as a function of IgG concentration (Figure 4.4b). The intensity was then converted to absorbance (A) by dividing the intensity (I) by the maximum signal for an 8-bit camera (I_o = 255) and subtracting it from 1. Next the absorbance of the control was defined as background and subtracted from the absorbance measured at

each concentration (Figure 4.4c). After the initial IgG infusion, all silica monolith test regions remain white to the naked eye and there is no significant difference in absorbance across different dilutions.
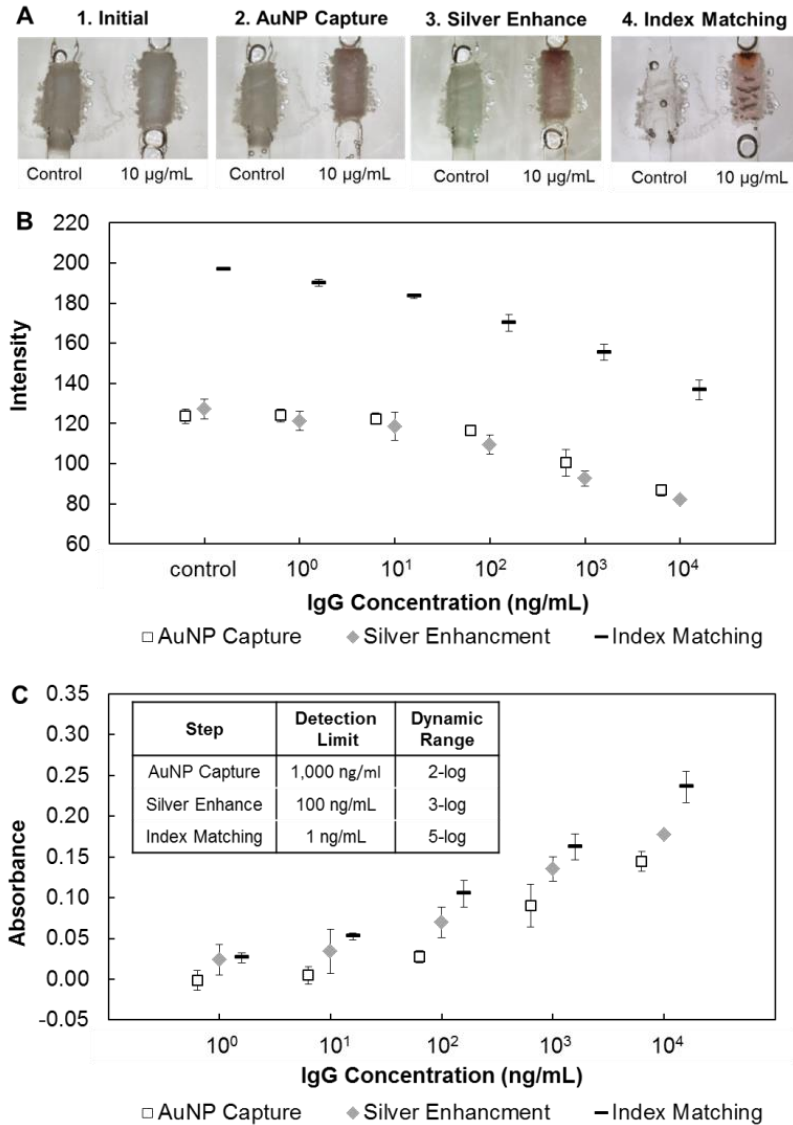
Figure 4.4: RGB images of the silica monolith detection elements are shown at time initial and after gold nanoparticle conjugate capture, silver enhancement, and refractive index matching with aqueous sucrose (A). The intensity (arbitrary units) of the detection region for different IgG concentrations is presented for reflectance based images after each assay step (B). The background corrected absorbance is shown for different IgG concentrations after each step (C). For each datum, n≥3 and error bars represent +/- 1 SD.

Following the introduction of AuIgG, detectable darkening of the monoliths was observed at the highest antibody concentrations, and a detection limit of 1 µg/mL was determined using the control absorbance plus 3 standard deviations as the noise floor with a 2 log dynamic range. After silver enhancement, the detection limit was reduced to 100 ng/mL with a commensurate increase in dynamic range to 3 logs. The formation of silver clusters was found to significantly increase the contrast in absorbance between the tested dilutions. Finally, the infusion of index matching solution was successful in further reducing the detection limit to 1 ng/mL or $1.2 *10^8$ antibodies, with a dynamic range of 5 logs achieved with measurement resolution of 1 log ($p < 0.05$). In comparison to planar based capture elements for metal enhanced gold nanoparticles the detection limit or assay time are significantly better than similar performing assays emphasizing the utility of a porous volumetric capture element (Figure 4.5). The observed increase in sensitivity and dynamic range is attributed to the ability of the index matching solution to reduce optical scattering within the porous monoliths, thereby allowing a greater portion of the porous silica volume to be accessible during optical detection. The results also confirm that the assay is quantitative, with optical signal for each IgG concentration tested found to be significantly different from other tested concentrations within the dynamic range using a student's t-test with p>0.05.
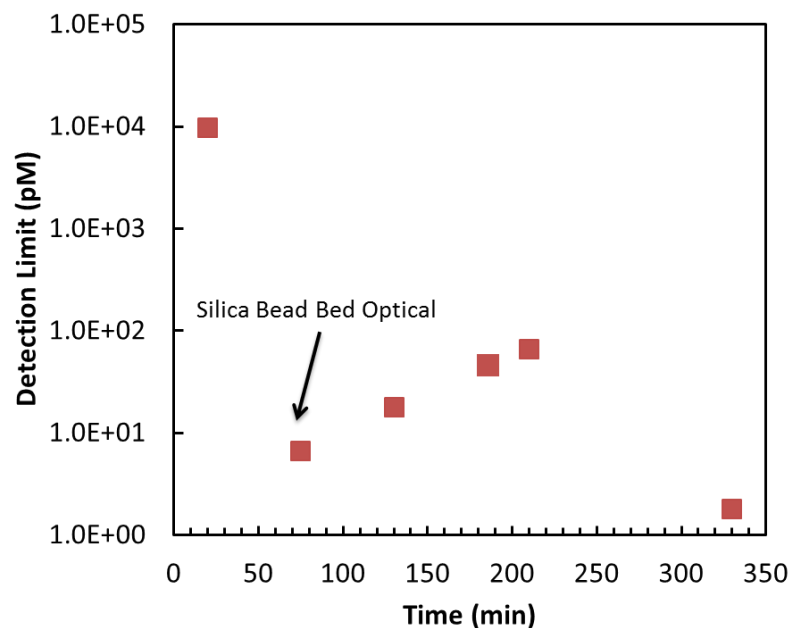
Figure 4.5: A comparison of detection limit vs. total assay completion time for sandwich immunoassays using optically based sensing with metallic enhancement of gold nanoparticle probes. All data points are for planar devices[33,38,74,98,99] with exception of the index matched silica bead bed used within this study.

These results emphasize the utility of both silver enhancement and index matching for the absorbance based assays to improve performance. Furthermore, the materials and reagents explored in this work are compatible with disposable diagnostic devices due to the low material and fabrication costs associated with thermoplastic microfluidics. The use of *ex situ* monoliths offers future potential for multiplexed assay development by functionalizing multiple porous silica monoliths for different target biomarkers before inserting them into the same microfluidic device. The results also suggest the ability to tailor the number of assay steps required based on the target biomarker concentration. For example for the detection of Norwalk virus, a common foodborne pathogen, measuring serum IgA concentrations on the order of 1-10 µg/mL is sufficient for diagnosis, potentially obviating the need for index matching.[100] In contrast, proteins such as cardiac troponin, a clinically important

biomarker of heart attack severity, must be measured at levels on the order of 1-10 ng/mL,[101] and thus would require that all assay steps be completed. In addition to the robustness and simplicity of the optical detection scheme employed here, the approach also supports integration with a portable photodetector and LED excitation source for use in remote or resource-limited environments.

4.5 Conclusions

This work demonstrates the use of *ex situ* functionalized porous silica monoliths within thermoplastic microchannels as a flexible method for sensitive immunoassays using a straightforward interrogation scheme based on optical absorbance measurements. The functionalized monolith structures were synthesized and conjugated to immunocapture probes in a batch process, ensuring economical fabrication as well as repeatability across devices that may be difficult or impossible to achieve using *in situ* detection element integration. The subsequent infusion of refractive index matching fluid facilitates the advantages of porous sensing elements, namely volumetric biomarker capture and rapid assay times, while minimizing light scattering that would otherwise compromise optical measurement sensitivity. Significantly, despite the additional assay step required to implement index matching, relatively short assay times were achieved with excellent sensitivity in the flow-through devices. Absorbance based immunoassays were completed in 50 min for a direct assay and 75 min for a sandwich assay, with detection limits between 1-10 ng/mL while the reflectance based sandwich immunoassay achieved a detection limit of 1 ng/mL and 5 logs of dynamic range in 75 min. The use of *ex situ* functionalized monoliths as discrete assay detection elements also suggest the potential to create

multiplexed assays by creating large batches of inserts for different target biomarkers before integration into the final microfluidic device. Future development applied to adapting these techniques to low cost POC devices for environmental monitoring or medical diagnostics may improve detection limits, allow quantification of dilute targets, and reduce total assay times compared to existing technology.

Chapter 5: Conclusions

5.1 Summary

In this dissertation multiple methods for implementing volumetric microfluidic detection elements was explored to enhance performance optical and impedemetric assays. By using volumetric detection elements instead of planar detection elements the density of biomarker capture probes is increased while decreasing characteristic diffusion lengths to reduce assay times and increase sensitivity compared to similar planar based assays. The demonstrated techniques utilize thermoplastics compatible with high-throughput production, stable commercial reagents, and simple measurement instrumentation compatible with point of care (POC) diagnostics development.

For an impedemetric assay (Chapter 2) a porous polymer monolith and a silica bead bed were used as volumetric detection elements in conjunction with gold interdigitated electrode arrays. A direct and sandwich assay were demonstrated by using silver enhanced immunogold conjugates (AuIgG) labels to decrease the measured volumetric impedance. For the direct assay a 3 log dynamic range was demonstrated using a polymer monolith and an array of 10 μm fingers spaced 15 μm apart. For a direct assay with electrode arrays spaced 15, 40, and 100 μm apart there was no significant difference in impedance change suggesting that the electrode spacing has minimal effect on sensor performance. Finally a sandwich immunoassay was performed with a detection limit of 10 ng/mL and a 4 log dynamic range using a silica bead bed and 10 μm wide fingers spaced 100 μm apart. The study demonstrates

the potential use of low resolution electrodes with microfluidic volumetric detection elements to achieve or better similar sensitivity to planar sensors that require high resolution electrodes and longer incubation times.

For optically based sensors (Chapters 3 and 4) that utilize porous volumetric detection elements we demonstrated the infusion of refractive index matching solutions to limit light scattering and enhance signal measurements. Enhancement of a fluorescent signal was shown using a porous polymer monolith and glycidal methacrylate index matching solution within a capillary for a direct immunoassay on the order of 1.5-2.5x. For a silica bead bed within a thermoplastic microchannel a transmission based immunoassay was completed using silver enhanced AuIgG and aqueous sucrose as an index matching solution. The detection limit for the direct immunoassay was 0.1 ng/mL with a 5 log dynamic range. Next a porous silica monolith element was synthesized and functionalized *ex situ* in a batch process before integration into a sealed thermoplastic microchannel by solvent bonding. A direct and sandwich immunoassay were completed using transmission based measurements with detection limits of 1-10 ng and 3-4 logs of dynamic range. For a sandwich immunoassay using reflectance based measurements the detection limit was 1 µg/mL after AuIgG capture, 100 ng/mL after silver enhancement, and 1 ng/ml after index matching with dynamic ranges of 2, 3, and 5 logs respectively. This detection limit and assay completion time is comparable to electrically based methods developed in this study and within literature. The use of *ex situ* elements suggests the potential for multiplexing using a batchwise process to create multiple detection elements for different biomarkers with consistent properties across devices. The flexible technique

enables the advantages or volumetric capture elements to create a quantitative assay with greater sensitivity and/or reduced assay times for POC diagnostics.

5.2 Contributions to Field

The development of techniques to utilize porous volumetric capture elements as an alternative to conventional planar capture surfaces has the potential to significantly improve the performance of microfluidic based assays by enhancing speed, sensitivity, and manufacturability of these devices. To explore the potential of this approach, two specific detection modes have been explored, namely impedance sensing and optical absorbance sensing.

In the case of impedance sensing, established microfluidic impedemetric sensors measure binding events on the planar electrodes of an interdigitated electrode array and/or on the microchannel surface. As a result, in order to achieve acceptable sensitivity the electrodes must be as close together as possible to maximize the electric field near the surface where the biorecognition events occur. Other methods to optimize sensitivity include long incubation times or silver enhancement with multiple sequential rinsing and enhancing steps to achieve high sensitivity without bridging the electrodes themselves. However by using porous volumetric detection elements the incubation and rinsing times required can be reduced given the high density of capture probes and shorter diffusion lengths that affect biorecognition events. Additionally the electrodes themselves can be spaced farther apart as the electric field does not need to be concentrated at the surface but can travel through the volume itself as long as the microchannel is sufficiently large enough. Thus cost

reduction can be achieved using lower resolution electrodes manufactured using high-throughput technologies without reducing detection performance.

The application of optical sensing to volumetric capture elements has been limited by the poor optical performance of porous media due to light scattering during measurement. A significant advance demonstrated in this work is the application of index matching as an approach to overcome this limitation. This work represents the first time that perfusion of a refractive index matching solution through a porous volumetric detection element in a microfluidic channel has been used to enhance optical signal by minimizing light scattering in the sensing region. In the present work, both detection limit and dynamic range were increased by 2 logs when employing an optimized protocol for refractive index matching. The index matching solution of aqueous sucrose is cost effective, simple to implement for POC applications, and is biocompatible in contrast to polar solvents or ionic solutions typically used for refractive index matching. The findings demonstrate that the combination of volumetric detection elements and fluidic index matching can enhance the speed, sensitivity, and dynamic range of microfluidic immunoassays. More generally, the technique is widely amenable to other applications that depend on optical characterization of high surface area porous volumetric elements within microfluidic platforms.

Finally the novel work on integration of *ex situ* functionalized porous volumetric silica elements into thermoplastic microchannels represents a contribution to the field. The use of *ex situ* elements facilitates lowering of production costs by functionalizing in a batch procedure that reduces reagents required and ensures

quality control not possible with *in situ* functionalized elements. Kendall et al. [64] previously demonstrated the *ex situ* functionalization of porous polymer substrates into solvent softened thermoplastic microchannels using a batchwise process to integrate uniform functional elements. The present work expands on this study by introducing porous silica elements with well characterized surface immobilization chemistries that are more compatible with index matching due to the greater pore size and hydrophilicity that supports easier perfusion of aqueous sucrose solutions. These silica elements synthesized with well characterized sol-gel chemistry have great potential for many fields including sensing and separation applications in thermoplastic microfluidic devices.

5.3 Future Work

The research presented in this dissertation sets a solid foundation for future studies using porous volumetric detection elements for microfluidics based POC assay development. For both the impedemetric and optical detection modalities demonstrated further work could enhance the utility of the techniques to the field and increase their overall impact.

For the impedemetric sensor the exploration of the choice of porous detection elements, assay methods, and integration with low cost measurement instrumentation could be explored. The use of a hydrophobic polymer monolith caused non-specific capture of gold nanoparticles, likely due to charge interactions, which resulted in higher signal levels from the negative control elements, and thus higher detection limits. By modifying the reagents, attempting different chemistries on the gold nanoparticle surface and polymer monolith surface, or modifying the detection

element material these non-specific interactions could be minimized, significantly improving future sensor performance. Similarly, the incubation times, reagent concentrations, and electrode configuration could be optimized and modeled to improve sensor performance for the desired detection limit and dynamic range. In addition the *in situ* UV polymerized polymer monoliths were found to exhibit significant variation across devices as the size, shape, pore morphology, and capture probe density achieved during reagent infusion were inconsistent. By using an *ex situ* fabrication and functionalization process, the consistency of the volumetric detection elements can be enhanced across devices. To address this, a silica bead bed was successfully employed to reduce non-specific interactions and improve measurement resolution. However, a more robust and manufacturable method employing alternative capture elements, such as silica monoliths, into thermoplastic microchannels without damaging the electrode arrays would improve the potential of these techniques. Finally the measurements presented utilized an expensive LCR meter controlled by a computer with LabVIEW software. Methods to introduce a miniaturized, hand-held impedance measurement device would greatly enhance the applicability to POC environments.

For the optical sensor methods, the addition of multiplexing capabilities, creation of more robust monolith integration techniques, and development of low cost imaging methods would enhance the relevance of the work to POC test development. In this dissertation only one detection element was integrated into a single thermoplastic microchannel. However using a batch process it is conceivable to functionalize a diverse array of *ex situ* elements with affinity for different biomarker

targets to achieve sensitive multiplex detection. By connecting the porous inserts in series there would be multiple detection regions without the need for any additional assay steps to diagnose a greater number of targets in the same amount of time. The silica inserts themselves are relatively brittle and handling them can result in damage that creates variability across devices. Methods to either handle the inserts more carefully such as disbursement in a fluid or encasing the porous silica monolith within a solid transparent shell such as a glass capillary could help this. For HPLC applications commercial silica monoliths within glass capillaries in a variety of sizes are sold by Millipore in their Chromolith[TM] product line demonstrating the commercial viability of this idea. Finally in the experiments shown here the optics and lighting used were large and constrained to a laboratory environment. However numerous studies utilizing either small microcontrollers connected to portable lighting and optical detectors or cell phone based imaging for POC assays demonstrate the feasibility of this technology.[50,102] Having a small handheld imaging device capable of signal processing would expand the possible applications of the technology to POC diagnostics.

Finally the demonstrated techniques should be used to analyze clinical samples for biomarkers of relevance to disease diagnosis. The immunoassays performed using generic IgG should be easily adapted to any antibody-antigen system with proper sample preparation methods. By integrating the detection elements with other technologies such as on-chip reagent storage, on-chip sample preparation, and miniaturized fluid actuation a truly portable assay can be created for use in POC diagnostics.

Bibliography

1. NIH. Point-of-Care Diagnostic Testing. 1–2 (2010).

2. Yager, P. *et al.* Microfluidic diagnostic technologies for global public health. *Nature* **442,** 412–8 (2006).

3. Dhawan, A. P. *et al.* Current and Future Challenges in Point-of-Care Technologies : A Paradigm-Shift in Affordable Global Healthcare With Personalized and Preventive Medicine. **3,** (2015).

4. American Academy of Microbiology. *Bringing the Lab to the Patient: Developing Point-of-Care Diagnostics for Resource Limited Settings*. (2011).

5. Manz, A., Graber, N. & Widmer, H. M. Miniaturized total chemical analysis systems: A novel concept for chemical sensing. *Sensors Actuators B Chem.* **1,** 244–248 (1990).

6. Auroux, P.-A., Iossifidis, D., Reyes, D. R. & Manz, A. Micro total analysis systems. 2. Analytical standard operations and applications. *Anal. Chem.* **74,** 2637–52 (2002).

7. H.Varmus, R. Klausner, E. Zerhouni, T.Acharya, A. S. Daar, P. A. S. Grand challenges in Global Health. *Science (80-.).* **302,** 398–399 (2003).

8. Daar, A. S. *et al.* Top ten biotechnologies for improving health in developing countries. *Nat. Genet.* **32,** 229–32 (2002).

9. Whitesides, G. M. The origins and the future of microfluidics. *Nature* **442,** 368–73 (2006).

10. Sharma, H., Nguyen, D., Chen, A., Lew, V. & Khine, M. Unconventional low-cost fabrication and patterning techniques for point of care diagnostics. *Ann. Biomed. Eng.* **39,** 1313–27 (2011).

11. Li, X., Ballerini, D. R. & Shen, W. A perspective on paper-based microfluidics: Current status and future trends. *Biomicrofluidics* **6,** 11301–1130113 (2012).

12. Geissler, M., Roy, E., Diaz-Quijada, G. A., Galas, J.-C. & Veres, T. Microfluidic patterning of miniaturized DNA arrays on plastic substrates. *ACS Appl. Mater. Interfaces* **1,** 1387–95 (2009).

13. Desai, D., Wu, G. & Zaman, M. H. Tackling HIV through robust diagnostics in the developing world: current status and future opportunities. *Lab Chip* **11,** 194–211 (2011).

14. Tsao, C.-W. & DeVoe, D. L. Bonding of thermoplastic polymer microfluidics. *Microfluid. Nanofluidics* **6,** 1–16 (2009).

15. Becker, H. & Gärtner, C. Polymer microfabrication technologies for microfluidic systems. *Anal. Bioanal. Chem.* **390,** 89–111 (2008).

16.   Ng, S. H. & Wang, Z. Hot roller embossing for the creation of microfluidic devices. *Symp. Des. Test, Integr. Packag. MEMS/MOEMS, DTIP 2008* 262–265 (2008). doi:10.1109/DTIP.2008.4752997

17.   Culbertson, C. T., Mickleburgh, T. G., Stewart-James, S. A., Sellens, K. A. & Pressnall, M. Micro total analysis systems: fundamental advances and biological applications. *Anal. Chem.* **86,** 95–118 (2014).

18.   Ahn, C. H. *et al.* Disposable Smart Lab on a Chip for Point-of-Care Clinical Diagnostics. *Proc. IEEE* **92,** 154–173 (2004).

19.   Yan, X.-F., Wang, M.-H. & Dong, A. Progress of Interdigitated Array Microelectrodes Based Impedance Immunosensor. *Chinese J. Anal. Chem.* **39,** 1601–1610 (2011).

20.   Gaster, R. S., Hall, D. A. & Wang, S. X. nanoLAB: an ultraportable, handheld diagnostic laboratory for global health. *Lab Chip* **11,** 950–6 (2011).

21.   Guan, J.-G., Miao, Y.-Q. & Zhang, Q.-J. Impedimetric biosensors. *J. Biosci. Bioeng.* **97,** 219–26 (2004).

22.   Prodromidis, M. I. Impedimetric immunosensors—A review. *Electrochim. Acta* **55,** 4227–4233 (2010).

23.   Towe, B. C. & Pizziconi, V. B. A microflow amperometric glucose biosensor. *Biosens. Bioelectron.* **12,** 893–9 (1997).

24.   Berggren, C., Stalhandske, P., Brundell, J. & Johansson, G. A feasibility study of a capacitive biosensor for direct detection of DNA hybridization. *Electroanalysis* **11,** 156–160 (1999).

25.   Min, J. & Baeumner, A. J. Characterization and Optimization of Interdigitated Ultramicroelectrode Arrays as Electrochemical Biosensor Transducers. *Electroanalysis* **16,** 724–729 (2004).

26.   Zou, Z., Kai, J. & Ahn, C. H. Electrical characterization of suspended gold nanowire bridges with functionalized self-assembled monolayers using a top-down fabrication method. *J. Micromechanics Microengineering* **19,** 055002 (2009).

27.   Radke, S. M. & Alocilja, E. C. A high density microelectrode array biosensor for detection of E. coli O157:H7. *Biosens. Bioelectron.* **20,** 1662–1667 (2005).

28.   Varshney, M., Li, Y., Srinivasan, B. & Tung, S. A label-free, microfluidics and interdigitated array microelectrode-based impedance biosensor in combination with nanoparticles immunoseparation for detection of Escherichia coli O157:H7 in food samples. *Sensors Actuators B Chem.* **128,** 99–107 (2007).

29.   Ramón-Azcón, J. *et al.* An impedimetric immunosensor based on interdigitated microelectrodes (IDmicroE) for the determination of atrazine residues in food samples. *Biosens. Bioelectron.* **23,** 1367–73 (2008).

30.   Zou, Z., Kai, J., Rust, M. J., Han, J. & Ahn, C. H. Functionalized nano interdigitated electrodes arrays on polymer with integrated microfluidics for

direct bio-affinity sensing using impedimetric measurement. *Sensors Actuators A Phys.* **136,** 518–526 (2007).

31. Breslauer, D. N., Maamari, R. N., Switz, N. A., Lam, W. A. & Fletcher, D. A. Mobile phone based clinical microscopy for global health applications. *PLoS One* **4,** e6320 (2009).

32. Yacoub-George, E. *et al.* Automated 10-channel capillary chip immunodetector for biological agents detection. *Biosens. Bioelectron.* **22,** 1368–75 (2007).

33. Chin, C. D. *et al.* Microfluidics-based diagnostics of infectious diseases in the developing world. *Nat. Med.* **17,** 1015–9 (2011).

34. Dineva, M. A., Mahilum-Tapay, L. & Lee, H. Sample preparation: a challenge in the development of point-of-care nucleic acid-based assays for resource-limited settings. *Analyst* **132,** 1193 (2007).

35. Mathews, S. T., Plaisance, E. P. & Kim, T. in *Methods Mol. Biol. Protein Blotting Detect.* (Kurien, B. T. & Scofield, R. H.) **536,** 499–513 (Humana Press, 2009).

36. Ellerbee, A. K. *et al.* Quantifying colorimetric assays in paper-based microfluidic devices by measuring the transmission of light through paper. *Anal. Chem.* **81,** 8447–52 (2009).

37. Kim, D. & Herr, A. E. Protein immobilization techniques for microfluidic assays. *Biomicrofluidics* **7,** 041501 (2013).

38. Wen, J., Shi, X., He, Y., Zhou, J. & Li, Y. Novel plastic biochips for colorimetric detection of biomolecules. *Anal. Bioanal. Chem.* **404,** 1935–44 (2012).

39. L. Malic, X. Zhang, D. Brassard, L. Clime, J. Daoud, C. Luebbert, V. Barrere, A. Boutin, S. Bidawid, J. Farber, N. C. Polymer-based microfluidic chip for rapid and efficient immunomagnetic capture and release of Listeria monocytogenes. *Lab Chip (in Prep.* **15,** 3994–4007 (2015).

40. Liu, J., Chen, C.-F., Chang, C.-W. & DeVoe, D. L. Flow-through immunosensors using antibody-immobilized polymer monoliths. *Biosens. Bioelectron.* **26,** 182–8 (2010).

41. De Jong, J., Lammertink, R. G. H. & Wessling, M. Membranes and microfluidics: a review. *Lab Chip* **6,** 1125–1139 (2006).

42. He, M. & Herr, A. E. Automated microfluidic protein immunoblotting. *Nat. Protoc.* **5,** 1844–1856 (2010).

43. Kendall, E. L. *et al.* Soft lithography microfabrication of functionalized thermoplastics by solvent casting. *J. Polym. Sci. Part B Polym. Phys.* n/a–n/a (2015). doi:10.1002/polb.23766

44. Peterson, D. S. Solid supports for micro analytical systems. *Lab Chip* **5,** 132–139 (2005).

45. Saarela, J. M. S., Heikkinen, S. M., Fabritius, T. E. J., Haapala, A. T. & Myllylä, R. A. Refractive index matching improves optical object detection in paper. *Meas. Sci. Technol.* **19,** 055710 (2008).

46. Saha, K., Agasti, S. S., Kim, C., Li, X. & Rotello, V. M. Gold nanoparticles in chemical and biological sensing. *Chem. Rev.* **112,** 2739–79 (2012).

47. Daniel, M. C. & Astruc, D. Gold Nanoparticles: Assembly, Supramolecular Chemistry, Quantum-Size-Related Properties, and Applications Toward Biology, Catalysis, and Nanotechnology. *Chem. Rev.* **104,** 293–346 (2004).

48. Posthuma-Trumpie, G. A., Korf, J. & van Amerongen, A. Lateral flow (immuno)assay: its strengths, weaknesses, opportunities and threats. A literature survey. *Anal. Bioanal. Chem.* **393,** 569–82 (2009).

49. Liu, R., Zhang, Y., Zhang, S., Qiu, W. & Gao, Y. Silver Enhancement of Gold Nanoparticles for Biosensing From Qualitative to Quantitative. *Appl. Spectrosc. Rev.* **49,** 121–138 (2014).

50. Laksanasopin, T. *et al.* A smartphone dongle for diagnosis of infectious diseases at the point of care. *Sci. Transl. Med.* **7,** 273re1 (2015).

51. Lei, K. F. & Wong, K. S. Automated Colorimetric Immunoassay Microsystem for Clinical Diagnostics. *Instrum. Sci. Technol.* **38,** 295–304 (2010).

52. Liu, Y., Zhang, D., Alocilja, E. C. & Chakrabartty, S. Biomolecules Detection Using a Silver-Enhanced Gold Nanoparticle-Based Biochip. *Nanoscale Res. Lett.* **5,** 533–538 (2010).

53. Yeh, C.-H., Huang, H.-H., Chang, T.-C., Lin, H.-P. & Lin, Y.-C. Using an electro-microchip, a nanogold probe, and silver enhancement in an immunoassay. *Biosens. Bioelectron.* **24,** 1661–6 (2009).

54. Lei, K. F. Electrical detection of sandwich immunoassay on indium tin oxide interdigitated electrodes. *Micro Nano Lett.* **6,** 157 (2011).

55. Yeh, C.-H., Wang, W.-T., Shen, P.-L. & Lin, Y.-C. A developed competitive immunoassay based on impedance measurements for methamphetamine detection. *Microfluid. Nanofluidics* **13,** 319–329 (2012).

56. Wiederoder, M. S. *et al.* Optical detection enhancement in porous volumetric microfluidic capture elements using refractive index matching fluids. *Analyst* **140,** 5724–5731 (2015).

57. Yang, L., Li, Y., Griffis, C. L. & Johnson, M. G. Interdigitated microelectrode (IME) impedance sensor for the detection of viable Salmonella typhimurium. *Biosens. Bioelectron.* **19,** 1139–47 (2004).

58. X, Z. & CH, A. Electrochemical determination of reversible redox species at interdigitated array micro/nanoelectrodes using charge injection method. in *IEEE Trans. Nanobioscience* 164–169 (2005).

59. Laczka, O., Baldrich, E., Muñoz, F. X. & del Campo, F. J. Detection of Escherichia coli and Salmonella typhimurium using interdigitated

microelectrode capacitive immunosensors: the importance of transducer geometry. *Anal. Chem.* **80,** 7239–47 (2008).

60. Van Gerwen, P. *et al.* Nanoscaled interdigitated electrode arrays for biochemical sensors. *Sensors Actuators B Chem.* **49,** 73–80 (1998).

61. Ooi, H. W. *et al.* Coordination complexes as molecular glue for immobilization of antibodies on cyclic olefin copolymer surfaces. *Anal. Biochem.* **456,** 6–13 (2014).

62. Fritzsche, W. & Taton, T. A. Metal nanoparticles as labels for heterogeneous, chip-based DNA detection. *Nanotechnology* **14,** R63–73 (2003).

63. Laksanasopin, T. *et al.* A smartphone dongle for diagnosis of infectious diseases at the point of care. *Sci. Transl. Med.* **7,** (2015).

64. Kendall, E. L., Wienhold, E., Rahmanian, O. D. & DeVoe, D. L. Ex Situ Integration of Multifunctional Porous Polymer Monoliths into Thermoplastic Microfluidic Chips. *Sens. Actuators. B. Chem.* **202,** 866–872 (2014).

65. Wallow, T. I. *et al.* Low-distortion, high-strength bonding of thermoplastic microfluidic devices employing case-II diffusion-mediated permeant activation. *Lab Chip* **7,** 1825–31 (2007).

66. Chen, C. F. *et al.* High-pressure needle interface for thermoplastic microfluidics. *Lab Chip* **9,** 50–5 (2009).

67. Wang, Z.-H. & Jin, G. Covalent immobilization of proteins for the biosensor based on imaging ellipsometry. *J. Immunol. Methods* **285,** 237–43 (2004).

68. Hacker, G. W. *et al.* Silver Acetate Autometallography : An Alternative Enhancement Technique for Immunogold-Silver Staining (IGSS) and Silver Amplification of Gold , Silver , Mercury and Zinc in Tissues. *J. Histotechnol.* **11,** 213–221 (1988).

69. Taton, T. A., Mirkin, C. A. & Letsinger, R. L. Scanometric DNA Array Detection with Nanoparticle Probes. *Science (80-.).* **289,** 1757–1760 (2000).

70. Brevnov, D. a. & Olson, T. S. Double-layer capacitors composed of interconnected silver particles and with a high-frequency response. *Electrochim. Acta* **51,** 1172–1177 (2006).

71. Shoar Abouzari, M. R., Berkemeier, F., Schmitz, G. & Wilmer, D. On the physical interpretation of constant phase elements. *Solid State Ionics* **180,** 922–927 (2009).

72. Maeng, J.-H. *et al.* A novel microfluidic biosensor based on an electrical detection system for alpha-fetoprotein. *Biosens. Bioelectron.* **23,** 1319–25 (2008).

73. Ko, Y.-J. *et al.* Real-time immunoassay with a PDMS–glass hybrid microfilter electro-immunosensing chip using nanogold particles and silver enhancement. *Sensors Actuators B Chem.* **132,** 327–333 (2008).

74. Yeh, C.-H., Hung, C.-Y., Chang, T. C., Lin, H.-P. & Lin, Y.-C. An immunoassay using antibody-gold nanoparticle conjugate, silver enhancement and flatbed scanner. *Microfluid. Nanofluidics* **6,** 85–91 (2008).

75. Daniel, J. Printed Electronics : Technologies , Challenges and Applications. in *Int. Work. Flex. Print. Electron. (IWFPE 10)* (2010).

76. Brabec, C. J. & Durrant, J. R. Solution-Processed Organic Solar Cells. *MRS Bull.* **33,** (2008).

77. Chin, C. D., Linder, V. & Sia, S. K. Commercialization of microfluidic point-of-care diagnostic devices. *Lab Chip* **12,** 2118–34 (2012).

78. Yager, P., Domingo, G. J. & Gerdes, J. Point-of-care diagnostics for global health. *Annu. Rev. Biomed. Eng.* **10,** 107–44 (2008).

79. Chen, C.-F., Liu, J., Chang, C.-C. & DeVoe, D. L. High-pressure on-chip mechanical valves for thermoplastic microfluidic devices. *Lab Chip* **9,** 3511–6 (2009).

80. Rahmanian, O., Chen, C.-F. & DeVoe, D. L. Microscale patterning of thermoplastic polymer surfaces by selective solvent swelling. *Langmuir* **28,** 12923–9 (2012).

81. Narang, U., Gauger, P. R., Kusterbeck, A. W. & Ligler, F. S. Multianalyte detection using a capillary-based flow immunosensor. *Anal. Biochem.* **255,** 13–19 (1998).

82. Mastichiadis, C. *et al.* Simultaneous determination of pesticides using a four-band disposable optical capillary immunosensor. *Anal. Chem.* **74,** 6064–6072 (2002).

83. Lane, S., West, P., François, A. & Meldrum, A. Protein biosensing with fluorescent microcapillaries. *Opt. Express* **23,** 7994–8006 (2015).

84. International Commission for Uniform Methods of Sugar Analysis. International refractive index scale of International Commission for Uniform Methods of Sugar Analysis (ICUMSA) for pure sucrose solutions at 20°C. (1974).

85. Budwig, R. Refractive index matching methods for liquid flow investigations. *Exp. Fluids* **17,** 350–355 (1994).

86. Yang, W.-J. *et al.* Quantification of microRNA by gold nanoparticle probes. *Anal. Biochem.* **376,** 183–8 (2008).

87. Yeh, C.-H., Hung, C.-Y., Chang, T. C., Lin, H.-P. & Lin, Y.-C. An immunoassay using antibody-gold nanoparticle conjugate, silver enhancement and flatbed scanner. *Microfluid. Nanofluidics* **6,** 85–91 (2008).

88. Liang, R.-Q., Tan, C.-Y. & Ruan, K.-C. Colorimetric detection of protein microarrays based on nanogold probe coupled with silver enhancement. *J. Immunol. Methods* **285,** 157–63 (2004).

89. Yang, M. & Wang, C. Label-free immunosensor based on gold nanoparticle silver enhancement. *Anal. Biochem.* **385,** 128–31 (2009).

90. Wang, Y. *et al.* Ultrasensitive colorimetric detection of protein by aptamer-Au nanoparticles conjugates based on a dot-blot assay. *Chem. Commun. (Camb).* 2520–2 (2008). doi:10.1039/b801055b

91. Ding, L., Qian, R., Xue, Y., Cheng, W. & Ju, H. In situ scanometric assay of cell surface carbohydrate by glyconanoparticle-aggregation-regulated silver enhancement. *Anal. Chem.* **82,** 5804–9 (2010).

92. Chin, C. D. *et al.* Microfluidics-based diagnostics of infectious diseases in the developing world. *Nat. Med.* **17,** 1015–1019 (2011).

93. Kurtinaitiene, B., Ambrozaite, D., Laurinavicius, V., Ramanaviciene, A. & Ramanavicius, A. Amperometric immunosensor for diagnosis of BLV infection. *Biosens. Bioelectron.* **23,** 1547–1554 (2008).

94. Rucker, V. C., Havenstrite, K. L. & Herr, A. E. Antibody microarrays for native toxin detection. *Anal. Biochem.* **339,** 262–270 (2005).

95. Ng, A. H. C., Uddayasankar, U. & Wheeler, A. R. Immunoassays in microfluidic systems. *Anal. Bioanal. Chem.* **397,** 991–1007 (2010).

96. Henares, T. G., Mizutani, F. & Hisamoto, H. Current development in microfluidic immunosensing chip. *Anal. Chim. Acta* **611,** 17–30 (2008).

97. Smith, J. H. *et al.* Chromatographic Properties of Silica-based Monolithic HPLC Columns. (2002).

98. Lin, H.-C., Wang, I.-L., Lin, H.-P., Chang, T. C. & Lin, Y.-C. Enhancement of an immunoassay using platinum nanoparticles and an optical detection. *Sensors Actuators B Chem.* **154,** 185–190 (2011).

99. Han, K. N. *et al.* Immunoassay of cardiac biomarkers using a photodiode array biochip. *Sensors Actuators, B Chem.* **207,** 470–476 (2015).

100. Kavanagh, O. *et al.* Serological responses to experimental Norwalk virus infection measured using a quantitative duplex time-resolved fluorescence immunoassay. *Clin. Vaccine Immunol.* **18,** 1187–1190 (2011).

101. Mahajan, V. S. & Jarolim, P. How to interpret elevated cardiac troponin levels. *Circulation* **124,** 2350–2354 (2011).

102. McRae, M. P. *et al.* Programmable bio-nano-chip system: a flexible point-of-care platform for bioscience and clinical measurements. *Lab Chip* **15,** 4020–4031 (2015).